Online Appendix for 'Shorting the Dollar When Global Stock Markets Roar: The Equity Hedging Channel of Exchange Rate Determination'

September 12, 2023

Abstract

This online appendix consists of the following four appendices: an appendix depicting a simple model that serves as theoretical motivation for the paper; two appendices detailing the Bayesian estimation procedures for the baseline and GIV- and Bartik-based econometric models, respectively; and an appendix presenting results from robustness checks for the baseline model's analysis.

Appendix A Theoretical Motivation

In what follows we lay out a simple structural framework which is meant to fix ideas and form a suitable conceptual base for our paper's empirical analysis. The framework is a partial equilibrium of the FX forward market consisting of two time periods (t and $t+1$) and three agents. The first is a local institutional investor (II) who sells foreign currency forwards so as to hedge its position in foreign equity markets. The second is a local importer (IM) who demands foreign currency forwards for its import activity. And the third is a global arbitrageur (GA) whose activity produces violations from CIP that are unaffected by foreign equity prices, in line with our empirical evidence.

We start our depiction of the model with a presentation of the supply side of the forward market by presenting the local II's supply of foreign currency forwards. We then show demand for foreign currency forwards by the local IM followed by an exposition of GA's activity. We end the section by defining equilibrium and presenting the model's main prediction.

A.1 Supply of Foreign Currency Forwards

Local II's Hedging. We assume that the local II hedges a share h of the FX risk of its period t foreign equity position, which we denote by A_t. (This position can be thought of as the product of some fixed quantity of foreign stocks and the price of these shocks.) In particular, this hedging is done by the local II through the selling of $FCF_{t,II} = hA_t$ foreign currency forwards on the forward market to the IM at FX forward rate $F_{t,t+1}$.

Local II's Supply of Foreign Currency Forwards. $FCF_{t,II} = hA_t$ represents local II's supply of foreign currency forwards. Note that this supply is perfectly inelastic given that it has no dependence on $F_{t,t+1}$. Importantly, a positive shock to global stock prices induces a rightward shift in the supply of foreign currency forwards because it produces a rise in A_t.

A.2 Demand for Foreign Currency Forwards

General Setting. The demand side of the forward market is governed by a local importer (IM) who buys in period t $FCF_{t,IM} = P_{t,W}Q_{t,IM}$ foreign currency forwards at forward rate $F_{t,t+1}$ to fund

the purchase of its imports of intermediate input quantity $Q_{t,IM}$ at foreign price $P_{t,W}$ (in foreign currency units).[1] It is effectively assumed here that the actual payment of this purchase will be made in period $t+1$ (i.e., the import deal is made with trade credit). The local IM's imported intermediate inputs are in turn used to produce and sell output quantity $M(Q_{t,IM})$ at local price $P_{t,L}$ (in local currency units) in the local economy, where $M(Q_{t,IM})$ is an increasing and concave function.

Local IM's Expected Profit. Given the setting described above, we can write local IM's profit as

$$\Pi_{t,IM} = P_{t,L}M(Q_{t,IM}) - P_{t,W}Q_{t,IM}F_{t,t+1}. \tag{A.1}$$

Optimal Demand for Foreign Currency Forwards. To derive the optimal demand for foreign currency forwards, we let the local IM maximize its expected profit from Equation (A.1) with respect to $Q_{t,IM}$. The solution to this maximization problem obtains local IM's optimal demand for imported intermediate inputs from which it is straightforward to compute the demand for foreign currency forwards $FCF_{t,IM} = P_{t,W}Q_{t,IM}$. The FOC of this problem is

$$P_{t,L}M'(Q_{t,IM}) = P_{t,W}F_{t,t+1}. \tag{A.2}$$

To see that the demand for foreign currency forwards is downward-sloping, we implicitly differentiate Equation (A.2) with respect to $F_{t,t+1}$ so as to obtain the first derivative of $Q_{t,IM}$ with respect to $F_{t,t+1}$ and then insert this derivative in the derivative of $FCF_{t,IM}$ with respect to $F_{t,t+1}$ to obtain the effect of the latter on the former:

[1] Our assumption that the IM is the local II's counterparty is backed by both unconditional and conditional evidence shown later in the paper. For simplicity, we assume that the local IM funds its import purchases entirely through the forward market. While it is possible to extend this framework to allow for some of the purchases to be made at the realized future spot rate, the latter simplifying perfect hedging assumption is consistent with the fact that the real sector in Israel has bought on a net basis over our sample period six times more foreign currency on the forward market than on the spot market, indicating that most of importers' FX flow activity takes place on the forward (rather than spot) market.

$$\frac{\partial Q_{t,IM}}{\partial F_{t,t+1}} = \frac{P_{t,W}}{P_{t,L}M''(Q_{t,IM})} < 0, \forall Q_{t,IM}, \tag{A.3}$$

$$\frac{\partial FCF_{t,IM}}{\partial F_{t,t+1}} = \frac{\partial\left\{P_{t,W}Q_{t,IM}\right\}}{\partial F_{t,t+1}} = \frac{P_{t,W}^2}{P_{t,L}M''(Q_{t,IM})} < 0, \forall Q_{t,IM}, \tag{A.4}$$

where the assumed concavity of M was used to establish the negative relation between $F_{t,t+1}$ and $Q_{t,IM}$, which in turn ensures the downward-sloping nature of the demand for foreign currency forwards. This constitutes an important result because it allows us to interpret the effect of a rise in A_t on the supply of foreign currency forwards (discussed in Section A.1) through the lens of a demand-supply framework in which a perfectly inelastic supply curve intersects a downward-sloping demand curve in the forward market. In particular, the prediction that a shock to global stock prices will produce a rightward shift in the (perfectly inelastic) supply of foreign currency forwards can now be interpreted as happening along a downward-sloping demand curve and thus will lead in equilibrium in the forward market to a rise in foreign currency forward flows along with a decline in the FX forward rate.

A.3 Global Arbitrageur

We now introduce into the model a global arbitrageur (GA) that facilitates the determination of the FX spot rate, which we denote by S_t. This facilitation is an outcome of the following cross-currency swap. (While left unmodeled, the counterparty to this swap trade can be thought of as a broker-dealer institution.) The GA buys spot $Q_{t,GA}$ foreign currency units and sells spot $Q_{t,GA}S_t$ local currency units while simultaneously buying forward $Q_{t,GA}S_t(1+i_{t+1,L})$ local currency units and selling $Q_{t,GA}(1+i_{t+1,W})$ foreign currency units at forward rate $F_{t,t+1}$ (with $i_{t+1,L}$ and $i_{t+1,W}$ representing the local and foreign risk-free interest rates, respectively).

Haircut. We follow Ivashina et al. (2015) and Liao and Zhang (2020) and assume that a haircut is applied to GA's swap trade in the amount of $\kappa Q_{t,GA}$, with $0 < \kappa < 1$. That is, the GA is required to deposit a share κ of its swap position to its (unmodeled) broker-dealer counterparty. This initial margin requirement constitutes a cost for the GA that is equal the foregone interest earnings that

it would be able to earn absent this requirement (i.e., $\kappa Q_{t,GA} i_{t+1,W}$). This haircut-induced cost has merit in producing a violation of CIP that accords with that we see in our data[2] in that it exists unconditionally but does not play a role in the equity hedging channel.

GA's Profit Maximization. We are now in position to write GA's profit from its arbitrage activity as

$$Q_{t,GA} \frac{S_t}{F_{t,t+1}} (1 + i_{t+1,L}) - Q_{t,GA} (1 + i_{t+1,W}) - \kappa Q_{t,GA} i_{t+1,W}. \tag{A.5}$$

The FOC that results from maximizing the profit from Equation (A.5) with respect to $Q_{t,GA}$ is

$$\frac{S_t}{F_{t,t+1}} (1 + i_{t+1,L}) = 1 + i_{t+1,W} + \kappa i_{t+1,W}, \tag{A.6}$$

where $\frac{S_t}{F_{t,t+1}} (1 + i_{t+1,L})$ represents the synthetic, CIP-implied foreign (gross) risk-free interest rate which is clearly higher than the actual one owing to the haircut-induced cost. In other words, Equation (A.6) implies a negative cross-currency basis that is caused by the swap trade's haircut-induced friction with this basis unaffected by A_t. Also noteworthy is the fact that this equation implies a positive relation between the FX spot rate and the FX forward rate; this is important for our purposes as it implies that in our model the sign (as well as magnitude in percentage terms) of the FX spot rate's response to changes in foreign equity prices is the same as that of the forward rate.

A.4 Model Equilibrium

We define equilibrium in the FX forward market as the equality $FCF_{t,II} = FCF_{t,IM} = FCF_t$, with FCF_t denoting the equilibrium level of FX forward flows and where $FCF_{t,II} = hA_t$ and $FCF_{t,IM} = P_{t+1,W} F_{t,t+1} Q_{t,IM}$. The latter two equations, integrated with the equilibrium condition $FCF_{t,II} = FCF_{t,IM} = FCF_t$, join the FOCs of the local IM's, and GA's problems (i.e., Equations (A.2), and (A.6)) in forming a system of four equations in four unknowns (FCF_t, $Q_{t,IM}$, $F_{t,t+1}$, and S_t) which represents our model's equilibrium.[3]

[2] This violation is of course not specific to our data given the robust finding from the post-GFC sample for various currencies on negative cross-currency basis with respect to the dollar (see, e.g., Du et al. (2018)).

[3] It is noteworthy that a proof that relies on a fixed-point argument for the existence and uniqueness of a solution to this four-equation system is available upon request from the authors.

Relation Between A_t and FCF_t, $F_{t,t+1}$, and S_t. A rise in A_t (as a result of a shock to global stock prices) implies a rightward shift in the perfectly inelastic supply of foreign currency forwards that takes place along a downward-sloping corresponding demand curve, where the latter is not affected by either A_t or h. This implies in turn that in equilibrium there must be a rise (fall) in quantity (price) of foreign currency forwards (i.e., a rise (fall) in FCF_t ($F_{t,t+1}$)).

Moreover, Since FOC (A.6) implies a positive and proportional relation between S_t and $F_{t,t+1}$ which is not dependent on A_t, the equilibrium prediction just noted for $F_{t,t+1}$ must also carry over to S_t (and in a one-to-one relation in percentage terms). Hence, in sum, we can deduce that a shock to global stock prices is predicted to reduce the spot rate in the same magnitude (in percentage terms) as it does the forward rate.

Appendix B Posterior Distribution of Parameters: Baseline Model

Given the block-recursiveness of the econometric model (Equations (1) and (2) from the text), we present the estimation algorithm separately for these two equations.

B.1 Equation (1)

Companion Form of Specification. Keeping with the notation from Section 5.2.1 of the paper, Equation (1) from the text can be written in companion form as follows:

$$Y = XB + U, \tag{B.1}$$

where $Y = [\Delta MSCI_1, ..., \Delta MSCI_T]'$, $X = [X_1, ..., X_T]'$, $X_t = [\Delta MSCI_{t-1}, ..., \Delta MSCI_{t-p}, 1]'$, $B = [B_1, ..., B_p, B_c]'$, and $U = [u_1, ..., u_T]'$ (with T being the time dimension of the sample and p being the number of lags). B here represents the reduced form coefficient vector of Equation (1) from the text and σ_u^2 is the variance of the reduced form innovation series u_t from that equation.

Specification of Uninformative Prior. We follow the conventional approach of specifying a normal-inverse Wishart prior distribution for the reduced-form parameters:[4]

$$vec(B) \mid \sigma_u^2 \sim N(vec(\bar{B}_0), \sigma_u^2 \otimes N_0^{-1}), \tag{B.2}$$

$$\sigma_u^2 \sim IW_1(v_0 S_0, v_0), \tag{B.3}$$

where N_0 is a $(p+1)$x$(p+1)$ positive definite matrix, S_0 is a scalar, and $v_o > 0$. As shown by Uhlig (1994), the latter prior implies the following posterior distribution:

$$vec(B) \mid \sigma_u^2 \sim N(vec(\bar{B}_T), \sigma_u^2 \otimes N_T^{-1}), \tag{B.4}$$

$$\sigma_u^2 \sim IW_1(v_T S_T, v_T), \tag{B.5}$$

where $v_T = T + v_0$, $N_T = N_0 + X'X$, $\bar{B}_T = N_T^{-1}(N_0 \bar{B}_0 + X'X\hat{B})$,
$S_T = \frac{v_0}{v_T} S_0 + \frac{T}{v_T}\hat{\sigma_u^2} + \frac{1}{v_T}(\hat{B} - \bar{B}_0)' N_0 N_T^{-1} X'X(\hat{B} - \bar{B}_0)$, $\hat{B} = (X'X)^{-1}X'Y$,
and $\hat{\sigma_u^2} = (Y - X\hat{B})'(Y - X\hat{B})/T$.

We follow the literature and use a weak prior, i.e., $v_0 = 0$, $N_0 = 0$, and arbitrary S_0 and $\bar{B}_0$. This implies that the prior distribution is proportional to σ_u^2 and that $v_T = T$, $S_T = \hat{\sigma_u^2}$, $\bar{B}_T = \hat{B}$, and $N_T = X'X$.

Posterior Simulator. In light of the above-described prior formulation, the posterior simulator for B and σ_u^2 can be described as follows:

1. Draw σ_u^2 from an $IW_1(T\hat{\sigma_u^2}, T)$ distribution.
2. Draw B from the conditional distribution $MN(\hat{B}, \sigma_u^2 \otimes (X'X)^{-1})$.
3. Repeat steps 1 and 2 a large number of times and collect the drawn B's and σ_u^2's.

Once we have these draws at hand, we compute the standardized MSCI index shock, which is the standardized residual from Equation (1) from the text and feed it into the estimation of Equation (2) from the text, as described next.

[4]Since Equation (1) from the text is univariate, the assumed inverse-Wishart distribution for σ_u^2 is denoted by IW_1, where the subscript 1 represents the univariate nature of Equation (1) from the text and its corresponding univariate inverse-Wishart distribution.

B.2 Equation (2)

Companion Form of Specification. Drawing on the notation from Section 5.2.1 of the paper, let the set of the parameters (coefficients matrix and residual standard deviation) to be estimated from Equation (2) from the text be given by Q_h and $\sigma_{\epsilon,h}$. Equation (2) from the text can then be written in companion form as follows:[5]

$$Y_h = X_h Q_h + \zeta_h, \tag{B.6}$$

where h is the regression's rolling horizon with $h = 0, ..., 500$; $Y_h = [y_h, y_{h+1}, ..., y_T]'$; $X_h = [X_1, ..., X_{T-h}]'$, with $X_t = [\hat{u}_t, 1]'$; $Q_h = [\Xi_h, \alpha_h]'$; and $\zeta_h = [\epsilon_h, ..., \epsilon_T]'$. Q_h here represents the coefficient matrix of Equation (2) from the text and $\sigma^2_{\epsilon,h}$ is the variance of ϵ_{t+h} (the residual from that equation).

Specification of Uninformative Prior. We assume the following normal-inverse Wishart prior distribution for these parameters:

$$vec(Q_h) \mid \sigma^2_{\epsilon,h} \sim N(vec(\bar{Q}_{0,h}), \sigma^2_{\epsilon,h} \times N_0^{-1}), \tag{B.7}$$

$$\sigma^2_{\epsilon,h} \sim IW_1(v_0 S_{0,h}, v_0), \tag{B.8}$$

where N_0 is a 2 x 2 positive definite matrix; S_0 is a variance scalar; and $v_o > 0$. As shown by Uhlig (1994), the latter prior implies the following posterior distribution:

$$vec(Q_h) \mid \sigma^2_{\epsilon,h} \sim N(vec(\bar{Q}_h), \sigma^2_{\epsilon,h} \times N_h^{-1}), \tag{B.9}$$

$$\sigma^2_{\epsilon,h} \sim IW_1(v_h S_h, v_h), \tag{B.10}$$

where $v_h = T - h + v_0$; $N_h = N_0 + X_h' X_h$; $\bar{Q}_h = N_h^{-1}(N_0 \bar{Q}_{0,h} + X_h' X_h \hat{Q}_h)$; $S_h = \frac{v_0}{v} S_{0,h} + \frac{T-h+1}{v_h} \hat{\sigma}^2_{\epsilon,h} + \frac{1}{v_h}(\hat{Q}_h - \bar{Q}_{0,h})' N_0 N_h^{-1} X_h' X_h (\hat{Q}_h - \bar{Q}_{0,h})$, where $\hat{Q}_h = (X_h' X_h)^{-1} (X_h)' Y$ and $\hat{\sigma}^2_{\epsilon,h} = (Y_h - X_h \hat{Q}_h)'(Y_h - X_h \hat{Q}_h)/(T-h)$.

[5] While there is, technically speaking, notational abuse of capital letters Y and X in Equations (B.1) and (B.6), what matters is that they are of course defined and used in the context of their corresponding equations and hence their specific contexts avoid expositional confusion. (The context for the first equation is a single equation while for the second it is a rolling regression context (hence the use of subscript h for Y in the second equation).)

We use a weak prior, i.e., $v_0 = 0$, $N_0 = 0$, and arbitrary $S_{0,h}$ and $\bar{Q}_{0,h}$. This implies that the prior distribution is proportional to $\sigma^2_{\epsilon,h}$ and that $v_h = I \times (T-h)$, $S_h = \hat{\sigma}^2_{\epsilon,h}$, $\bar{Q}_h = \hat{Q}_h$, and $N_h = X_h' X_h$. Due to the temporal correlations of the error term ϵ_{t+h}, the likelihood function is misspecified which in turn requires that the residual variance estimate $\hat{\sigma}^2_{\epsilon,h}$ be appropriately modified so as to improve estimation precision (Müller (2013)). Toward this end, we apply a Newey-West correction to $\hat{\sigma}^2_{\epsilon,h}$ which accounts for arbitrary temporal correlation of the error term and denote the corrected variance estimate by $\hat{\sigma}^2_{\epsilon,h,hac}$.

Posterior Simulator. Given the above-described prior formulation and the correction to $\hat{\sigma}^2_{\epsilon,h}$, we are now in position to lay out the posterior simulator for Q_h and $\sigma^2_{\epsilon,h}$, which accounts for uncertainty in the estimation of the MSCI index shock series $\hat{u}_t$ and can be described as follows:

1. Do Steps 1-3 from the posterior simulator of Equation (1) from the text and obtain $\hat{u}_t$ (whose standardized value is to be used as explanatory variable for the next two steps).
2. Draw $\sigma^2_{\epsilon,h}$ from an $IW_1((T-h+1)\hat{\sigma}^2_{\epsilon,h,hac}, (T-h+1))$ distribution.
3. Draw Q_h from the conditional distribution $MN(\hat{Q}_h, \sigma^2_{\epsilon,h} \times (X_h' X_h)^{-1})$.
4. Repeat Steps 1-3 a large number of times and collect the drawn Q_h's and $\sigma^2_{\epsilon,h}$'s.

B.3 Smoothing of Impulse Responses

The high-frequency nature of our data combined with our local projection estimation approach produce rather jagged raw impulse responses. It is therefore important and warranted to smooth the raw impulse responses with a data-dependent smoothing procedure that suitably integrates into our Bayesian framework. We now turn to present this procedure.

General Setting and Objective. Let $\Theta = [\Xi_1, \Xi_2, ..., \Xi_{500}]'$ denote the raw impulse response 500×1 vector. The posterior simulator of Steps 1-4 shows how to obtain posterior draws for this vector and hence effectively gives knowledge of its posterior probability distribution $\mathbb{P}(\Theta \mid data)$.

We assume the following smooth trend, state-space model for Ξ_h (with h representing the horizon):

$$\Xi_h = \tilde{\Xi}_h + \eta_h, \tag{B.11}$$

$$\tilde{\Xi}_h = 2\tilde{\Xi}_{h-1} - \tilde{\Xi}_{h-2} + \gamma_h, \tag{B.12}$$

where Equation (B.11) is the model's measurement equation and Equation (B.12) is the model's state equation; $\tilde{\Xi}_h$ is the smoothed impulse response at horizon h whose first-difference follows a random walk with shock γ_h, which is a zero-mean independently and identically normally distributed variable with variance σ_γ; and η_h is a zero-mean independently and identically normally distributed variable with variance σ_η which represents the noise embodied in the raw impulse response function (IRF). Letting $\tilde{\Theta} = [\tilde{\Xi}_1, \tilde{\Xi}_2, ..., \tilde{\Xi}_{500}]'$ denote the smoothed impulse response 500×1 vector, our main interest and objective can be described as lying in simulating $\tilde{\Theta}$ from its posterior probability distribution $\mathbb{P}(\tilde{\Theta} \mid data)$.

Relation of Model (B.11)-(B.12) to HP-Filter. The smooth trend, state-space model from Equations (B.11)-(B.12) can be viewed as a model-based interpretation of Hodrick and Prescott (1997)'s popular HP-filter (see, e.g., Harvey (1990), Gómez (1999), and Appendix D from Cornea-Madeira (2017)). Specifically, the MSE-optimal smoothed $\tilde{\Xi}_h$ obtained from applying the Kalman filter to this model to find the values for σ_η and σ_γ that maximize the likelihood function for Θ ($\mathbb{P}(\Theta \mid \sigma_\eta, \sigma_\gamma, data)$) corresponds to the HP-filter of Ξ_h with smoothing parameter $\frac{\sigma_\eta^2}{\sigma_\gamma^2}$.[6] In this sense, the way we model the smoothed IRF follows the general suggestion from Plagborg-Møller (2016) to smooth raw impulse responses with the HP-filter.[7]

[6] Hamilton (2018) uses this maximum likelihood estimation procedure for several popular macro time series and finds very low values for the smoothing parameter (see his Table 1), which constitutes an important underlying evidence for his criticism against using the HP-filter and the validity of the assumptions that underlie its estimation. However, his criticism pertains to using the HP-filter for *macro time series*, not IRFs. Hence, his work should not be viewed through the lens of an estimation framework seeking to smooth impulse responses. Accordingly, and in contrast to his estimates for macro time series, our estimated posterior distribution for the smoothing parameter for the non-informative prior case is rather tightly centered around very high smoothing parameters.

[7] Plagborg-Møller (2016) puts forward a classical estimation procedure that selects a shrinkage smoothing parameter that minimizes the unbiased risk estimate (URE) object, which was shown by Plagborg-Møller (2016) to be an asymptotically uniformly unbiased estimator of MSE of the smoothed impulse response estimates relative to the raw ones. What is particularly appealing about the HP-filter-based smoothing approach for our setting is that it optimally smoothes an *estimated* impulse response function; hence,

Treatment of Hyperparamters σ_η and σ_γ. To simulate posterior draws of $\tilde{\Theta}$, we need to simulate posterior draws from the joint posterior probability distribution of Θ, σ_η, and σ_γ, $\mathbb{P}(\Theta, \sigma_\eta, \sigma_\gamma \mid data)$, and then use the Kalman filter smoother to obtain posterior draws of $\tilde{\Theta}$. Bayes' law dictates that $\mathbb{P}(\Theta, \sigma_\eta, \sigma_\gamma \mid data) = \mathbb{P}(\sigma_\eta, \sigma_\gamma \mid \Theta, data)\mathbb{P}(\Theta \mid data)$ and that $\mathbb{P}(\sigma_\eta, \sigma_\gamma \mid \Theta, data) \propto \mathbb{P}(\Theta \mid \sigma_\eta, \sigma_\gamma, data)\mathbb{P}(\sigma_\eta, \sigma_\gamma \mid data)$.

Since we have knowledge of $\mathbb{P}(\Theta \mid data)$ from the previous section's estimation, all we need in order simulate posterior draws from $\mathbb{P}(\Theta, \sigma_\eta, \sigma_\gamma \mid data)$ is to know $\mathbb{P}(\sigma_\eta, \sigma_\gamma \mid \Theta, data)$. Following the approach of Giannone et al. (2015) and Miranda-Agrippino and Ricco (2021), we treat σ_η and σ_γ as additional model parameters for which we specify a bivariate uniform prior probability distribution and estimate them via the Kalman filter as the maximizers of the posterior likelihood $\mathbb{P}(\sigma_\eta, \sigma_\gamma \mid \Theta, data)$, in the spirit of hierarchical modeling. Our assumed flat prior for the joint prior distribution of σ_η and σ_γ (conditional on the observed data), $\mathbb{P}(\sigma_\eta, \sigma_\gamma \mid data)$, implies equivalency between maximizing $\mathbb{P}(\Theta \mid \sigma_\eta, \sigma_\gamma, data)$ and $\mathbb{P}(\sigma_\eta, \sigma_\gamma \mid \Theta, data)$ (with respect to σ_η and σ_γ). We now turn to discuss the informativeness of our flat prior as implied by the limit we impose on the upper bound of σ_γ's support.

Informativeness of Flat Prior $\mathbb{P}(\sigma_\eta, \sigma_\gamma \mid data)$. IRFs from theoretical macroeconomic models tend to be either monotonic or hump-shaped, i.e., they normally have at most one inflection point (see, e.g., Alvarez and Lippi (2022)). Accordingly, it is sensible to discipline the support of $\mathbb{P}(\sigma_\eta, \sigma_\gamma \mid data)$ on which their joint uniform prior is defined in a way that restrains the possibility of the smoothed IRF having more than one inflection point. Since the number of times an IRF's slope changes its sign determines its number of inflection points, and since the bigger σ_γ the more likely the IRF's slope changes sign, a natural way to do this restraining is by limiting the upper bound of σ_γ such that $\tilde{\Xi}_{j,h} - \tilde{\Xi}_{j,h-1}$ changes its sign at most once for all considered horizons. In what follows we elucidate the two-step procedure we use to set this upper bound for each poste-

we can conveniently use it within our Bayesian estimation framework as explained in this section. Two additional proposed smoothing procedures for local projections that have been recently put forward are Barnichon and Brownlees (2019)'s frequentist B-spline smoothing estimation procedure and Tanaka (2019)'s Bayesian B-spline smoothing estimation procedure; however, both are effectively generalized ridge estimation procedures that are not directly applied to the standard raw estimated impulse responses, thus rendering them void of the HP-filter based appealing feature mentioned above in the context of our Bayesian setting.

rior draw of Ξ_h.

First, for each posterior draw of $\Xi_{j,h}$, we perform an unconstrained Kalman filter estimation of Model (B.11)-(B.12) which provides us with estimates of σ_η and σ_γ that we denote by $\sigma_{\eta,MLE}$ and $\sigma_{\gamma,MLE}$, respectively. Second, we form a grid of 100 equally-spaced values ranging from $\frac{\sigma_{\gamma,MLE}}{99}$ to $\sigma_{\gamma,MLE}$ and, for each posterior draw of Ξ_h, we simulate via the Kalman filter 500 smoothed IRFs for $\sigma_{\eta,MLE}$ and $\sigma_\gamma \in [\frac{\sigma_{\gamma,MLE}}{99}, \sigma_{\gamma,MLE}]$. We search over the latter grid for values of σ_γ for which at least one of the corresponding simulated 500 smoothed impulse responses functions' slope changes its sign more than once and take the smallest such value to be the upper bound of σ_γ's prior distribution's support; if no such value is found then $\sigma_{\gamma,MLE}$ is taken to be the latter upper bound.[8]

Estimation of $\mathbb{P}(\tilde{\Theta} \mid data)$. We are now in position to describe the estimation of the posterior distribution of the smoothed IRF $\tilde{\Theta}$. As noted on Page 10, this posterior distribution can be obtained from $\mathbb{P}(\Theta, \sigma_\eta, \sigma_\gamma \mid data)$ by using the Kalman filter smoother to produce $\tilde{\Theta}$ from the posterior draws of Θ, σ_η, and σ_γ.

In particular, for each posterior draw of Θ from posterior simulator 1-4, we conduct a *constrained* Kalman filter estimation of Model (B.11)-(B.12) where parameter σ_γ is constrained to be between 0 and the upper bound obtained from the procedure described on Page 11 (σ_η is unconstrained, merely restricted to be non-negative); this constrained Kalman filter estimation provides us with estimates of σ_η and σ_γ which we then feed into the Kalman filter smoother to produce a smoothed IRF. Applying this smoothing procedure to the 500 posterior draws of raw IRFs results in the sought after posterior distribution of smoothed IRFs.

[8] Our approach is in the spirit of the recommendation from Plagborg-Møller (2019) to choose IRF smoothness hyperparameters by trial-and-error simulations. It is noteworthy that using a non-informative prior does not alter the baseline message of our paper but it does often produce more than one IRF slope sign change for most considered variables in our analysis and this, as discussed above, does not accord with the rather pervasively smooth nature of macroeconomic models' IRFs.

Appendix C Posterior Distribution of Parameters: GIV-Based Model

The appendix presents the details of the estimation and inference procedure for the GIV-based model from Equations (3) and (4) from the text. Given the block-recursiveness of this econometric model, we present the estimation algorithm separately for these two equations. These equations are shown again below:

$$FF_{i,t} = \alpha_{i,0} + \beta_{i,1}FF_{i,t-1} + \cdots + \beta_{i,p_i}FF_{i,t-p_i} + C_{i,0}Z_t + ... + C_{i,p_i}Z_{t-p_i} + \xi_{i,t}, \tag{C.1}$$

$$y_{t+h} - y_{t-1} = \alpha_{2,h} + \Phi_h\hat{\omega}_t + v_{t+h}, \tag{C.2}$$

For future reference, let the stacked K_ix1 $B_i = [\alpha_{i,0}, ..., C_{i,p_i}]'$ (K_i is the number of parameters for the RHS of Equation (C.1) corresponding to the ith II) and 2x1 $Q_h = [\alpha_{2,h}, \Phi_h]'$ matrices represent the coefficient matrices from Equations (C.1) and (C.2), respectively. I.e., the parameters to be estimated from these two equations can be summarized by coefficient matrices B_is and residual variance $\sigma^2_{i,\xi}$ for Equation (C.1) and coefficient matrix Q_h and residual variance $\sigma^2_{v,h}$ for Equation (C.2).

C.1 Equation (C.1)

Companion Form of Specification. Keeping with the above notation, Equation (C.1) can be written in companion form as follows:

$$Y_i = X_iB_i + \Gamma_i, \tag{C.3}$$

where i indexes IIs and $Y_i = [FF_{i,1}, ..., FF_{i,T}]'$, $X = [X_{i,1}, ..., X_{i,T}]'$, $X_{i,t} = [1, ..., Z_{i,t-p_i}]'$, $B = [\alpha_{i,0}, ..., C_{i,p_i}]'$, and $\Gamma_i = [\xi_{i,1}, ..., \xi_{i,T}]'$ (with T being the time dimension of the sample and p_i being the number of lags). B_i here represents the reduced form coefficient vector of Equation (C.1) and $\sigma^2_{i,\xi}$ is the variance of the reduced form innovation series $\xi_{i,t}$ from that equation.

Specification of Uninformative Prior. We follow the conventional approach of specifying a normal-inverse Wishart prior distribution for the reduced-form parameters:[9]

$$vec(B_i) \mid \sigma^2_{i,\xi} \sim N(vec(\bar{B}_0), \sigma^2_{i,\xi} \otimes N_0^{-1}), \tag{C.4}$$

$$\sigma^2_{i,\xi} \sim IW_1(v_0 S_0, v_0), \tag{C.5}$$

where N_0 is a KxK positive definite matrix (K is the number of parameters for the RHS of Equation (C.1)), S_0 is a scalar, and $v_o > 0$. As shown by Uhlig (1994), the latter prior implies the following posterior distribution:

$$vec(B_i) \mid \sigma^2_{i,\xi} \sim N(vec(\bar{B}_{i,T}), \sigma^2_{i,\xi} \otimes N_{i,T}^{-1}), \tag{C.6}$$

$$\sigma^2_{i,\xi} \sim IW_1(v_T S_{i,T}, v_T), \tag{C.7}$$

where $v_T = T + v_0$, $N_{i,T} = N_0 + X_i' X_i$, $\bar{B}_{i,T} = N_{i,T}^{-1}(N_0 \bar{B}_0 + X_i' X_i \hat{B}_i)$,
$S_{i,T} = \frac{v_0}{v_T} S_0 + \frac{T}{v_T} \hat{\sigma^2}_{i,\xi} + \frac{1}{v_T}(\hat{B}_I - \bar{B}_0)' N_0 N_{i,T}^{-1} X_i' X_i (\hat{B}_i - \bar{B}_0)$, $\hat{B}_i = (X_i' X_i)^{-1} X_i' Y_i$,
and $\hat{\sigma^2}_{i,\xi} = (Y_i - X_i \hat{B}_i)'(Y_i - X_i \hat{B}_i)/T$.

We follow the literature and use a weak prior, i.e., $v_0 = 0$, $N_0 = 0$, and arbitrary S_0 and $\bar{B}_0$. This implies that the prior distribution is proportional to $\sigma^2_{i,\xi}$ and that $v_T = T$, $S_{i,T} = \hat{\sigma^2}_{i,\xi}$, $\bar{B}_{i,T} = \hat{B}_i$, and $N_{i,T} = X_i' X_i$.

Posterior Simulator. In light of the above-described prior formulation, the posterior simulator for B_i and $\sigma^2_{i,\xi}$ can be described as follows:

1. Draw $\sigma^2_{i,\xi}$ from an $IW_1(T\hat{\sigma^2}_{i,\xi}, T)$ distribution.
2. Draw B_i from the conditional distribution $MN(\hat{B}_i, \sigma^2_{i,\xi} \otimes (X_i' X_i)^{-1})$.
3. Repeat steps 1 and 2 a large number of times and collect the drawn B_i's and $\sigma^2_{i,\xi}$'s.[10]

Once we have these draws at hand, we compute the standardized aggregate shock to IIs' forward supply, which is the difference between the size-weighted- and inverse-variance-weighted-average of the II-specific residuals from Equation (C.1) for the GIV shock case and the mean of

[9] Since Equation (3) from the text is univariate, the assumed inverse-Wishart distribution for σ^2_{ξ} is denoted by IW_1, where the subscript 1 represents the univariate nature of Equation (3) from the text and its corresponding univariate inverse-Wishart distribution.

[10] We generate 500 such posterior draws.

these residuals for Bartik shock case (both shocks are standardized to have a unit variance), and feed it into the estimation of Equation (C.2), as described next.

C.2 Equation (C.2)

Companion Form of Specification. Drawing on the above notation, let the set of the parameters (coefficients matrix and residual standard deviation) to be estimated from Equation (C.2) be given by Q_h and $\sigma_{v,h}$. This equation (8) can then be written in companion form as follows:[11]

$$Y_h = X_h Q_h + \zeta_h, \tag{C.8}$$

where h is the regression's rolling horizon with $h = 0, ..., 500$; $Y_h = [y_h - y_{-1}, y_{h+1} - y_0, ..., y_T - y_{T-h-1}]'$; $X_h = [X_1, ..., X_{T-h}]'$, with $X_t = [1, \hat{\omega}_t]'$ (where $\hat{\omega}_t = \sum_{i=1}^{14} \hat{\xi}_{i,t}$); $Q_h = [\alpha_{2,h}, \Phi_h]'$; and $\zeta_h = [v_h, ..., v_T]'$. Q_h here represents the coefficient matrix of Equation (C.2) from the text and $\sigma^2_{v,h}$ is the variance of v_{t+h} (the residual from that equation).

Specification of Uninformative Prior. We assume the following normal-inverse Wishart prior distribution for these parameters:

$$vec(Q_h) \mid \sigma^2_{v,h} \sim N(vec(\bar{Q}_{0,h}), \sigma^2_{v,h} \times N_0^{-1}), \tag{C.9}$$

$$\sigma^2_{v,h} \sim IW_1(v_0 S_{0,h}, v_0), \tag{C.10}$$

where N_0 is a 2 x 2 positive definite matrix; S_0 is a variance scalar; and $v_o > 0$. As shown by Uhlig (1994), the latter prior implies the following posterior distribution:

$$vec(Q_h) \mid \sigma^2_{v,h} \sim N(vec(\bar{Q}_h), \sigma^2_{v,h} \times N_h^{-1}), \tag{C.11}$$

$$\sigma^2_{v,h} \sim IW_1(v_h S_h, v_h), \tag{C.12}$$

where $v_h = T - h + v_0$; $N_h = N_0 + X_h' X_h$; $\bar{Q}_h = N_h^{-1}(N_0 \bar{Q}_{0,h} + X_h' X_h \hat{Q}_h)$; $S_h = \frac{v_0}{v} S_{0,h} + \frac{T-h+1}{v_h} \hat{\sigma}^2_{v,h} + \frac{1}{v_h}(\hat{Q}_h - \bar{Q}_{0,h})' N_0 N_h^{-1} X_h' X_h (\hat{Q}_h - \bar{Q}_{0,h})$, where $\hat{Q}_h = (X_h' X_h)^{-1} (X_h)' Y$ and $\hat{\sigma}^2_{v,h} = (Y_h - X_h \hat{Q}_h)'(Y_h - X_h \hat{Q}_h)/(T - h)$.

[11] While there is, technically speaking, notational abuse of capital letters Y and X in Equations (C.3) and (C.8), what matters is that they are of course defined and used in the context of their corresponding equations and hence their specific contexts avoid expositional confusion. (The context for the first equation is a single equation while for the second it is a rolling regression context (hence the use of subscript h for Y in the second equation).)

We use a weak prior, i.e., $v_0 = 0$, $N_0 = 0$, and arbitrary $S_{0,h}$ and $\bar{Q}_{0,h}$. This implies that the prior distribution is proportional to $\sigma^2_{v,h}$ and that $v_h = I \times (T-h)$, $S_h = \hat{\sigma}^2_{v,h}$, $\bar{Q}_h = \hat{Q}_h$, and $N_h = X_h' X_h$. Due to the temporal correlations of the error term v_{t+h}, the likelihood function is misspecified which in turn requires that the residual variance estimate $\hat{\sigma}^2_{v,h}$ be appropriately modified so as to improve estimation precision (Müller (2013)). Toward this end, we apply a Newey-West correction to $\hat{\sigma}^2_{v,h}$ which accounts for arbitrary temporal correlation of the error term and denote the corrected variance estimate by $\hat{\sigma}^2_{v,h,hac}$.

Posterior Simulator. Given the above-described prior formulation and the correction to $\hat{\sigma}^2_{u,h}$, we are now in position to lay out the posterior simulator for Q_h and $\sigma^2_{v,h}$, which accounts for uncertainty in the estimation of the aggregate forward supply shock series $\hat{\omega}_t = \sum_{i=1}^{14} \hat{\xi}_{i,t}$ and can be described as follows:

1. Do Steps 1-3 from the posterior simulator of Equation (C.1) and obtain $\hat{\omega}_t$ (whose standardized value is to be used as explanatory variable for the next two steps).
2. Draw $\sigma^2_{v,h}$ from an $IW_1((T-h+1)\hat{\sigma}^2_{v,h,hac}, (T-h+1))$ distribution.
3. Draw Q_h from the conditional distribution $MN(\hat{Q}_h, \sigma^2_{v,h} \times (X_h' X_h)^{-1})$.
4. Repeat Steps 1-3 a large number of times and collect the drawn Q_h's and $\sigma^2_{v,h}$'s.[12]

Finally, we apply the smoothing procedure described in Section B.3 to Φ_h to obtain the smoothed impulse responses to the forward supply shock.

Appendix D Robustness Checks

This section examines the robustness of the baseline results from the text (presented in Figure 4-8) along four dimensions. First, estimating the foreign equity innovation from micro data on IIs' regional portfolio weights by constructing from this data a properly aggregated foreign equity return for IIs. Second, replacing the MSCI return series with the S&P 500 index return series.

[12]The number of posterior draws is 500, as this posterior simulator generates a posterior draw for each of the 500 drawn forward supply shocks from the estimation of Equation (C.1).

Third, truncating the baseline sample at 2/19/2020 so as to exclude the COVID-19 period.[13] And fourth, altering the lag specification underlying the MSCI index regression. The presentation of all of the results follows the same exposition and structure underlying the baseline results from Figures 5-9 from the text.

D.1 Using IIs' Actual Foreign Equity Portfolio Return

One concern arising from our baseline MSCI return series, from which we identify the foreign equity innovation, is that this series may not be a good proxy for the actual return of IIs' foreign equity portfolio. To address this concern, we turn to BOI micro II-level data on regional portfolio weights. In particular, we construct each II's (there are a total of 116 such IIs, comprising the universe of Israeli IIs) foreign equity portfolio return using its regional portfolio weights and then aggregate the micro return into an aggregate return using IIs' foreign equity shares of IIs' aggregate foreign equity position. We then estimate our baseline model using the latter aggregate return series instead of the MSCI return series. Before turning to present the results from this exercise, we discuss four caveats to this micro-based foreign equity return series as well as report and discuss the correlation between the latter series and the baseline MSCI return series.

Caveats. There are four caveats to using the micro-based series of this section that are noteworthy. First, the micro data underlying this series only begins from 11/3/2015, i.e., there is a loss of seven years of observations stemming from the use of this series. Second, there is also a meaningful lack of data along the cross-sectional dimension with more than 40% of the II-level regional weight data missing. Third, the II-level regional portfolio weights do not pertain only to foreign equity holding weights but also represents holding of other asset types. Fourth, there is an average weight of 24.1% of IIs' foreign asset portfolios that is not allocated to any specific region because this share represents IIs' holding of global exchange traded funds whose specific regional holding weights are not identified by the BOI when constructing the regional weight shares.[14] We

[13] Global stock markets reached a peak on 2/19/2020, after which the COVID-induced bear market began to take place.

[14] An average 56.8% weight of IIs' foreign asset holdings is allocated to the U.S.; an average 12.9% weight is allocated to Europe; an average 2.8% weight is allocated to Australia; an average 2.7% weight is allocated to BRIC (Brazil, Russia, India, and China); and an average 1.5% weight is allocated to Asia. The stock

therefore allocate this residual share to the MSCI ACWI Index (our baseline MSCI index).

While these four caveats are noteworthy, they do not devoid the value of this robustness check. There is still a major share of data availability (roughly 60%) across the cross-sectional dimension, with large IIs' regional weight data availability being the central driver of this overall availability, which renders the aggregate micro-based return series a useful measure of the actual aggregate foreign equity portfolio return of the universe of Israeli IIs. And making the somewhat crude (albeit arguably reasonable) assumption that foreign equity and non-equity portfolio weights are not meaningfully different by region alleviates the concern that our treatment of foreign *asset* weights as proxying for foreign *equity* weights produces meaningful bias in the construction of IIs' foreign equity returns.

Relation Between Micro-Based Return and MSCI Return Series. The above-mentioned caveats, and especially the one related to the large loss of sample size along the time dimension, provide a reasoning against using the micro-based foreign equity return series as the baseline specification case. But, on their own, they do not warrant the use of the MSCI return series as the baseline specification case. Only a strong correlation between these two return series would warrant the use of the MSCI series as the baseline specification case since such strong correlation would suggest that the MSCI return series captures well the actual aggregate return on IIs' foreign equity portfolio.

Such warranting is indeed born out by the data. The correlation between the MSCI return series and the micro-based foreign equity return series is 97.2%. And this overwhelmingly strong correlation is not an artifact of the fact that an average 24.1% weight of the latter series is attached to the MSCI return series. Omitting this weight altogether from the construction of the micro-based foreign equity return series results in a foreign equity return series that has a similar and overwhelmingly strong correlation of 94.7% with the MSCI series. Hence, in sum, we can deduce that our baseline MSCI return series effectively represents the actual aggregate return on IIs' foreign equity portfolio while having the added advantage of being available for the entire sample

market return we use for the U.S. is the S&P 500 return; for Europe we use the MSCI Europe index; for Australia we use the S&P/ASX 200 index; for BRIC we use the MSCI BRIC Index; and for Asia we use the MSCI AC Asia Pacific Index.

availability of IIs' forward flow data.

Estimation Results. Figures D.1-D.5 present the results from replacing the baseline MSCI return series with the micro-based foreign equity return series. These figures follow the same exposition and structure as the baseline figures from the text (Figures 5-9). It is clear that the significant exchange rate appreciation and IIs' short dollar position build up that were observed from the baseline case, in tandem with economically insignificant responses of interest rate differentials and cross-currency basis, also carry through to this section's estimation. Given the very strong correlation between the baseline MSCI return series and the micro-based return series underlying these figures, the results from the latter not only demonstrate a general insensitivity of our baseline results to modifying the baseline MSCI return series but also indicate that our baseline results carry through even when omitting the first 7 years from the baseline sample.

D.2 Replacing MSCI Return Series with S&P 500 Return Series

An additional reasonable alternative to the baseline MSCI return series we use in the paper is the S&P 500 return series. While IIs' average foreign asset portfolio weight allocated to the U.S. is 56.8%, leaving meaningful room for non-U.S. foreign equity holdings, the centrality of the widely and closely followed S&P 500 index in global stock markets warrants confirming that using this index does not invalidate our baseline results. (The correlation between the S&P 500 index return series and the micro-based return of IIs' foreign equity portfolio is 97.4%.[15] And the correlation between the S&P 500 return series and the baseline MSCI return series is 90%.)

Toward this end, Figures D.6-D.10 present the results from replacing the baseline MSCI return series with the S&P 500 return series. These figures follow the same exposition and structure as the baseline figures from the text (Figures 5-9). The message from the baseline results continues to hold also for this specification: there is a significant exchange rate appreciation and short position build up on the part of IIs, taking place in tandem with economically insignificant responses of interest rate differentials and cross-currency basis.

[15]This very high correlation is not merely driven by the 56.8% U.S. weight underlying IIs' foreign asset portfolio. Even after omitting this U.S. weight, the correlation between the micro-based return and the S&P 500 return is still considerably high at 82%.

D.3 Excluding the COVID-19-Period

While the COVID-19-related period clearly provides increased volatility to our baseline sample and thus has the potential of improving identification of the equity hedging channel, one may also argue that its uniqueness makes the case for showing that the baseline results are not driven by its inclusion. Toward this end, Figures D.11-D.15 present the results from truncating the baseline sample at February 19, 2020. These figures follow the same exposition and structure as the baseline figures from the text (Figures 5-9). It is clear that the baseline message of the paper does not change from exclusion of the COVID-19-related period, with the MSCI index innovation continuing to induce significant exchange rate appreciation and a coincident significant build up of short position on the dollar from IIs while producing economically insignificant responses of interest rate differentials and cross-currency basis. It is noteworthy that now, as opposed to the baseline case, the banking sector no longer serves as a significant long position holder - the real sector is the sole long position holder opposite of IIs.

Moreover, that the magnitude of the short position build up does appear to be larger for the baseline sample than for the pre-COVID sample possibly indicates that hedging activity of IIs was stronger in the COVID-related period than in the rest of the sample. This is to be expected given the considerable global stock market boom that followed the COVID-induced (short-lived) bear market. But hedging is still significant also in the pre-COVID sample with 33.9% of the short position's two-year variation being accounted for by the MSCI innovation. And, importantly, the latter innovation continues to explain a meaningful share of the variation in the spot rate, accounting for as much as 36% of its variation. It is noteworthy that this FEV share is even moderately higher than the baseline one.

One last noteworthy observation from this section's results is the insignificant selling of spot dollars seen from Figure D.12a, where there is actually significant buying of such dollars after 293 days (albeit not in very economically significant amounts). That there is significant selling of dollar forwards in tandem with no such selling of spot dollars, with the MSCI innovation explaining as much as 36% of the variation in the spot rate, bolsters confidence in the claim that what our estimation approach mainly picks up in the data is coming from an equity hedging channel rather

than a portfolio-rebalancing-induced spot market based mechanism.

D.4 Lag Specification

As noted in Footnote 13 from the text, optimal lag selection tests pointed to a 20-lag specification for Equation (1) from the text. Nevertheless, it is worthwhile to confirm that increasing or lowering the number of lags does not change our baseline results.

Toward this end, we have rerun our estimation of our model with 10 and 30 lags in Equation (1) from the text instead of the baseline 20-lag specification. The results for these alternative lag specifications are shown in Figures D.16-D.20 and Figures D.21-D.25, respectively, with the exposition and structure underlying these figures being the same as in the corresponding baseline figures from the text (Figures 5-9). Clearly, the results are both quantitatively and qualitatively similar to the baseline ones, with the MSCI index innovation inducing significant exchange rate appreciation and a significant build up of short position on the dollar while generating economically insignificant responses of interest rate differentials and cross-currency basis.

Figure D.1: **Impulse Responses to a One Standard Deviation Foreign Equity Innovation: Foreign Equity and Interest Rates: Replacing MSCI Return with a Micro-Based Foreign Equity Return**.

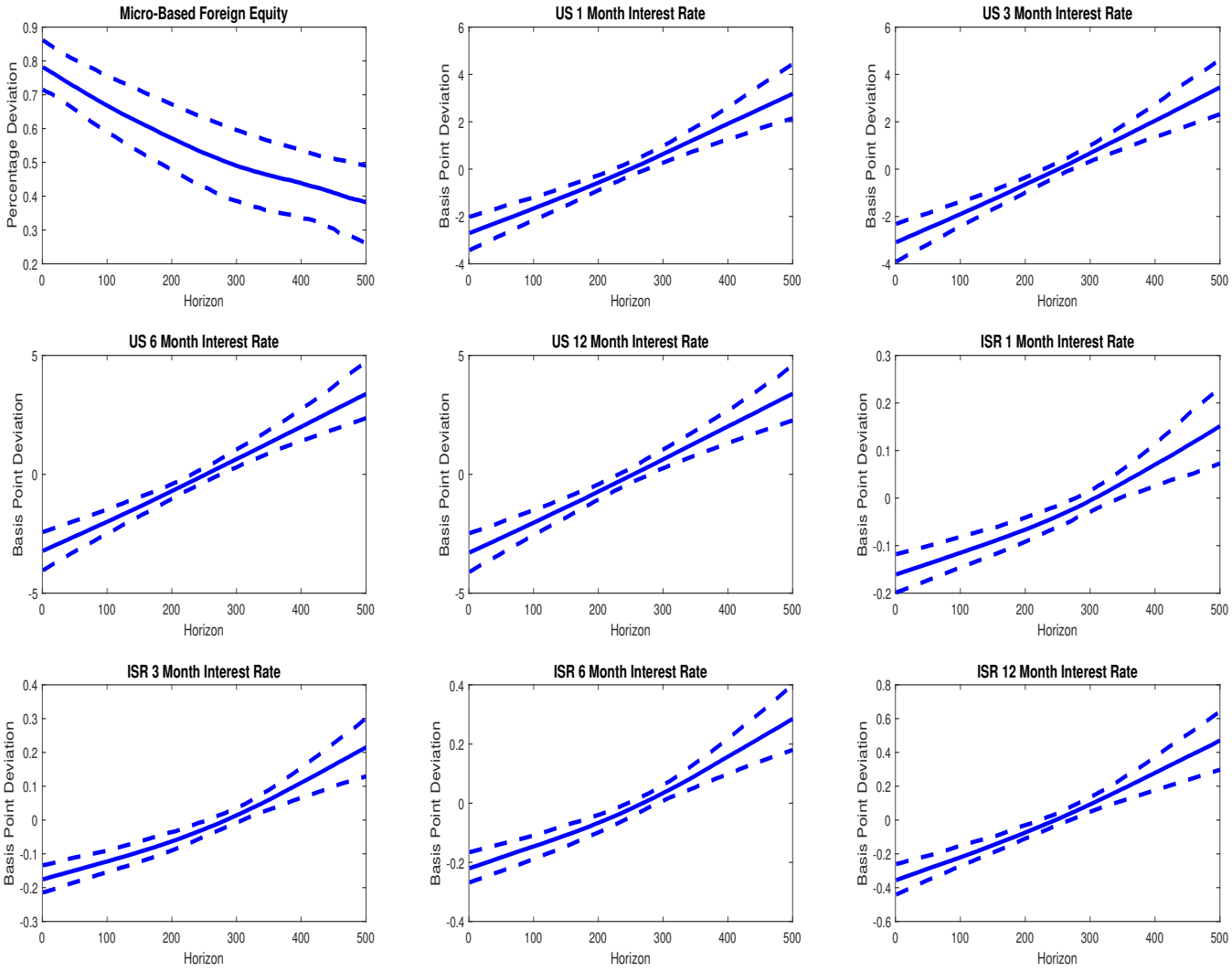

Notes: This figure presents the impulse responses of the micro-based foreign equity return (in accumulated form) from Section D.1 and 1-, 3-, 6-, and 12-month U.S. (Libor) and Israeli (Telbor) interest rates to a one standard deviation foreign equity innovation from replacing MSCI return with the micro-based foreign equity return in the model described by Equations (1) and (2) from the text. Responses are in terms of deviations from pre-shock values (percentage deviation for foreign equity and basis point deviation for interest rates). Horizon (on x-axis) is in days.

Figure D.2: **FX Market Prices and Quantities: Replacing MSCI Return with a Micro-Based Foreign Equity Return: (a) Impulse Responses; (b) FEVs**.

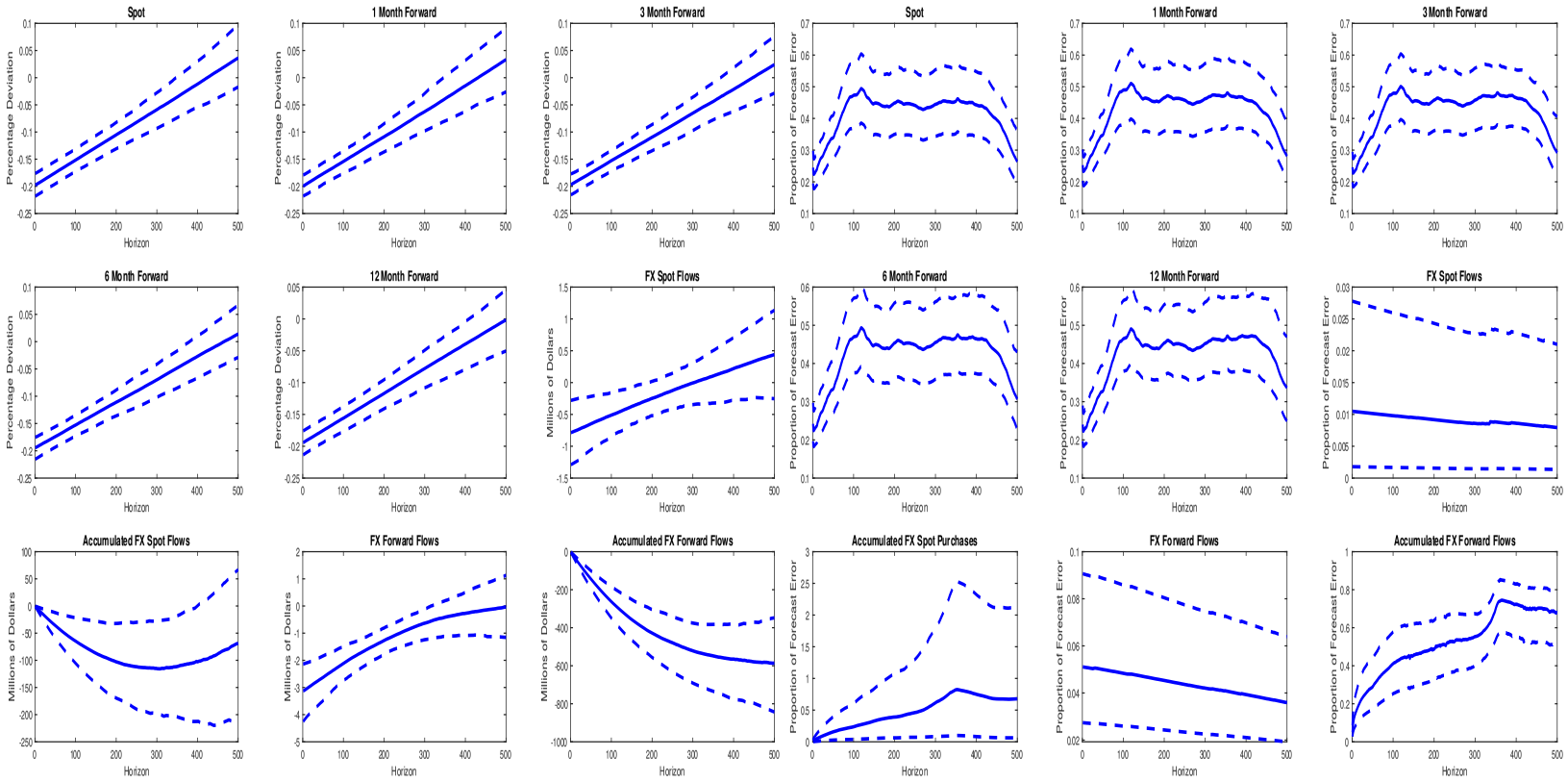

(a) Impulse Responses of FX Market Prices and Quantities to a One Standard Deviation MSCI Index Innovation.

(b) FEV of FX Market Prices and Quantities Attributable to MSCI Index Innovation.

Notes: Panel (a): This figure presents the impulse responses of the spot and forward rates and quantities to a one standard deviation foreign equity innovation from replacing MSCI return with the micro-based foreign equity return in the model described by Equations (1) and (2) from the text. Responses are in terms of deviations from pre-shock values (percentage deviation for spot and forward rates and Millions of dollars for spot and forward flows' raw and accumulated responses). Horizon (on x-axis) is in days. Panel (b): This figure presents the FEV share of the spot and forward rates and quantities that is attributable to the foreign equity innovation. Horizon is in days.

Figure D.3: **Impulse Responses to a One Standard Deviation MSCI Index Innovation: Replacing MSCI Return with a Micro-Based Foreign Equity Return: Non-II Sectors' Spot and Forward Flows**.

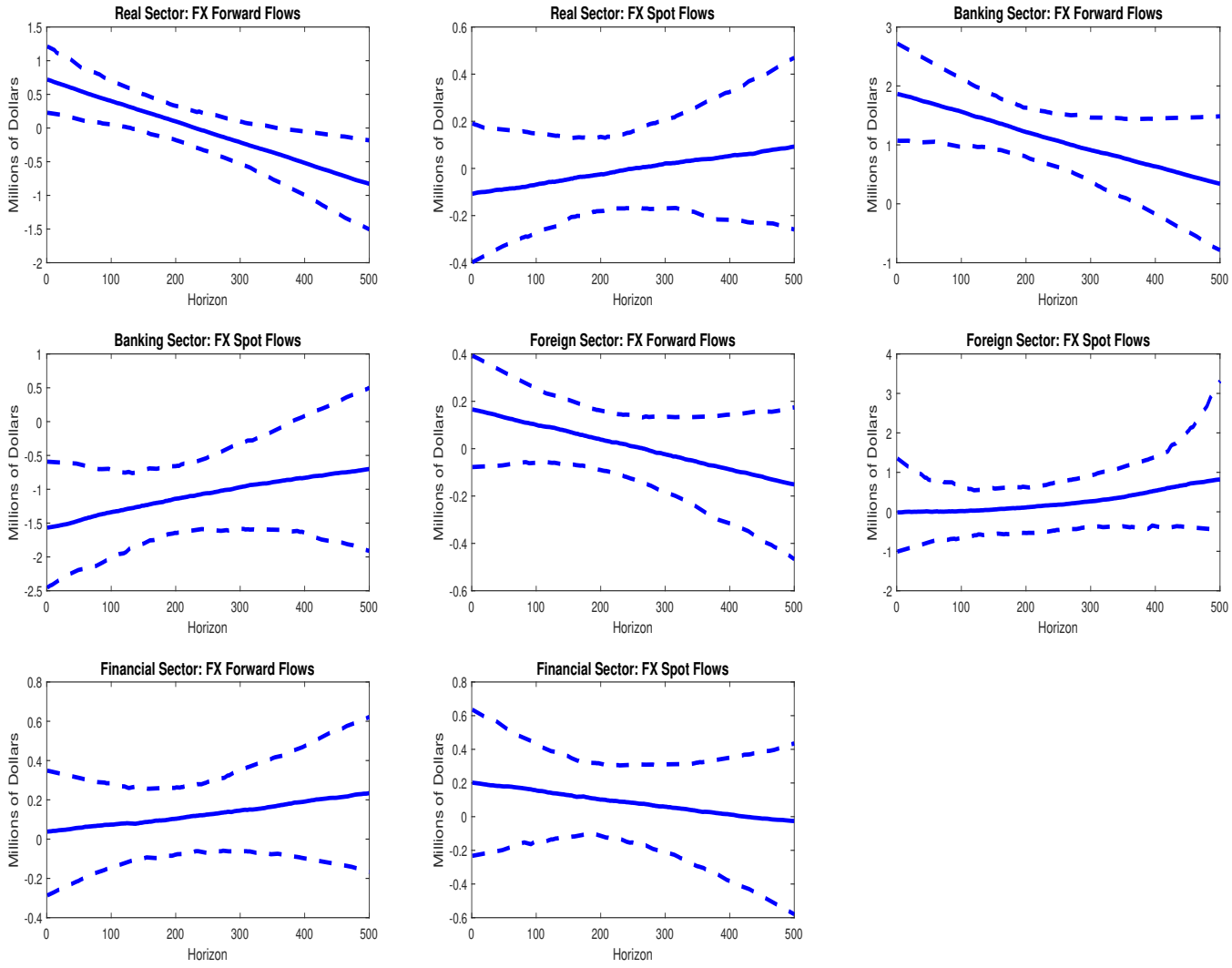

Notes: This figure presents the impulse responses of spot and forward flows of the real, banking, foreign, and financial sectors to a one standard deviation foreign equity innovation from replacing MSCI return with the micro-based foreign equity return in the model described by Equations (1) and (2) from the text. Responses are in terms of deviations from pre-shock values (in million of dollar terms). Horizon (on x-axis) is in days.

Figure D.4: **Impulse Responses to a One Standard Deviation MSCI Index Innovation: Replacing MSCI Return with a Micro-Based Foreign Equity Return: Banking and Real Sectors' Forward Flows Versus IIs' Forward Flows**.

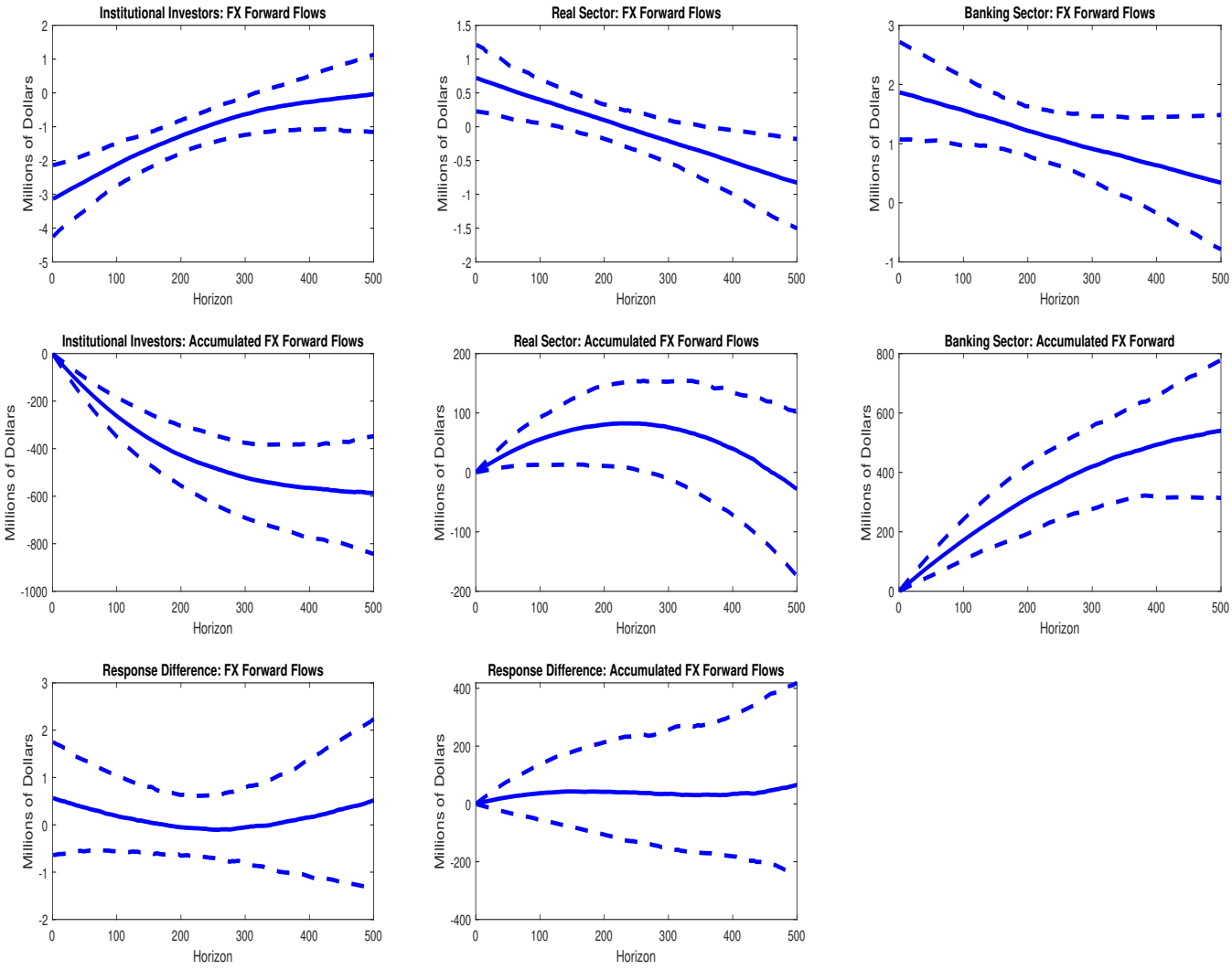

Notes: This figure presents the difference between raw and accumulated (in absolute terms) response of IIs' forward flows and the summed responses of the banking and real sectors' raw and accumulated forward flows, respectively, to a one standard deviation foreign equity innovation from replacing MSCI return with the micro-based foreign equity return in the model described by Equations (1) and (2) from the text. (For completeness, responses themselves (both raw and accumulated) for all three sectors are also shown in the figure.) Responses are in terms of deviations from pre-shock values (in million of dollar terms). Horizon (on x-axis) is in days.

Figure D.5: **Impulse Responses to a One Standard Deviation MSCI Index Innovation: Replacing MSCI Return with a Micro-Based Foreign Equity Return: Interest Rate Spreads and Cross-Currency Basis**.

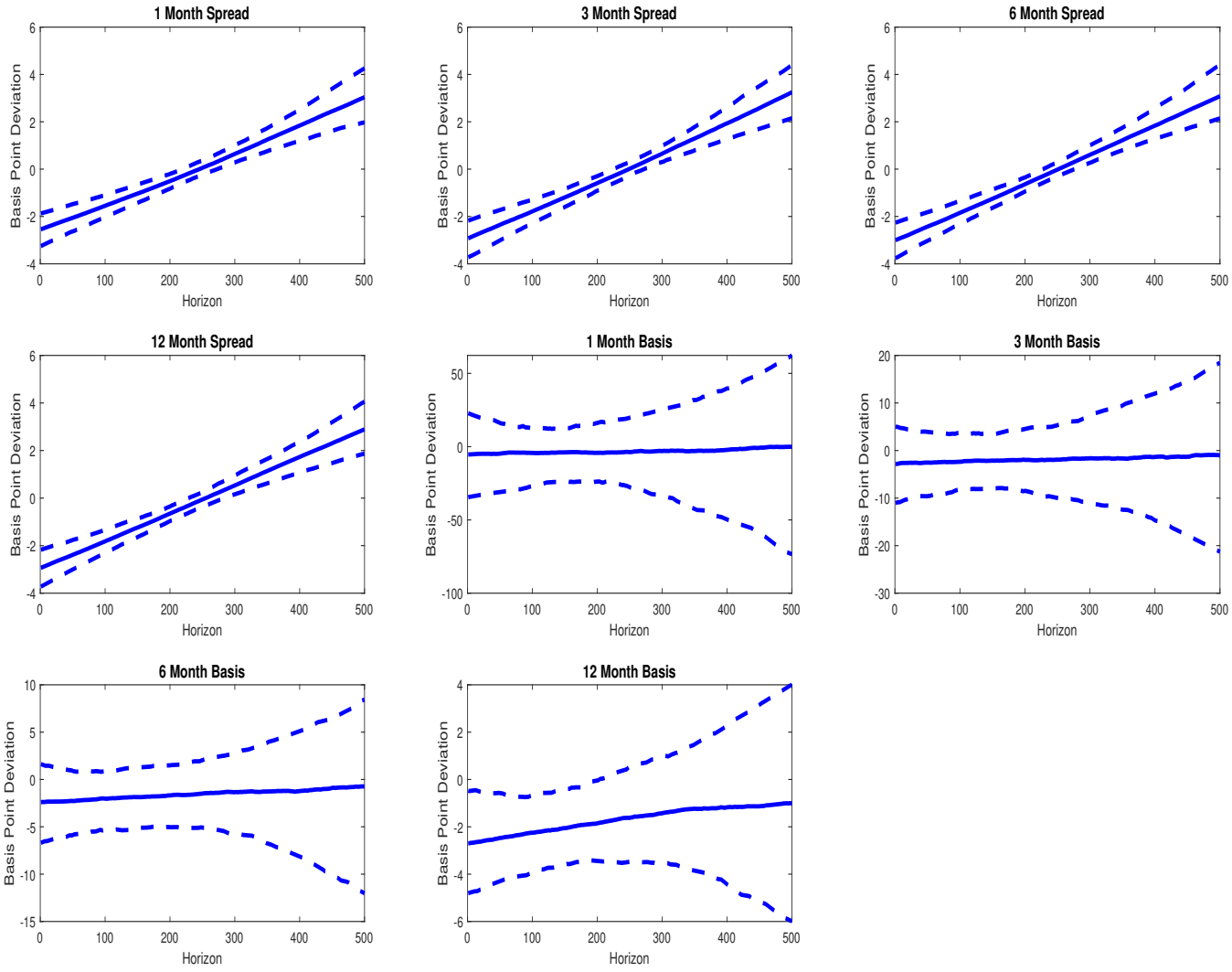

Notes: This figure presents the impulse response differences across U.S. (Libor) and Israeli (Telbor) interest rate responses and the associated USD/ILS cross-currency basis responses to a one standard deviation foreign equity innovation from replacing MSCI return with the micro-based foreign equity return in the model described by Equations (1) and (2) from the text. Responses are in terms of basis point deviation from pre-shock values. Horizon is in days.

Figure D.6: **Impulse Responses to a One Standard Deviation S&P 500 Index Innovation: S&P 500 and Interest Rates**.

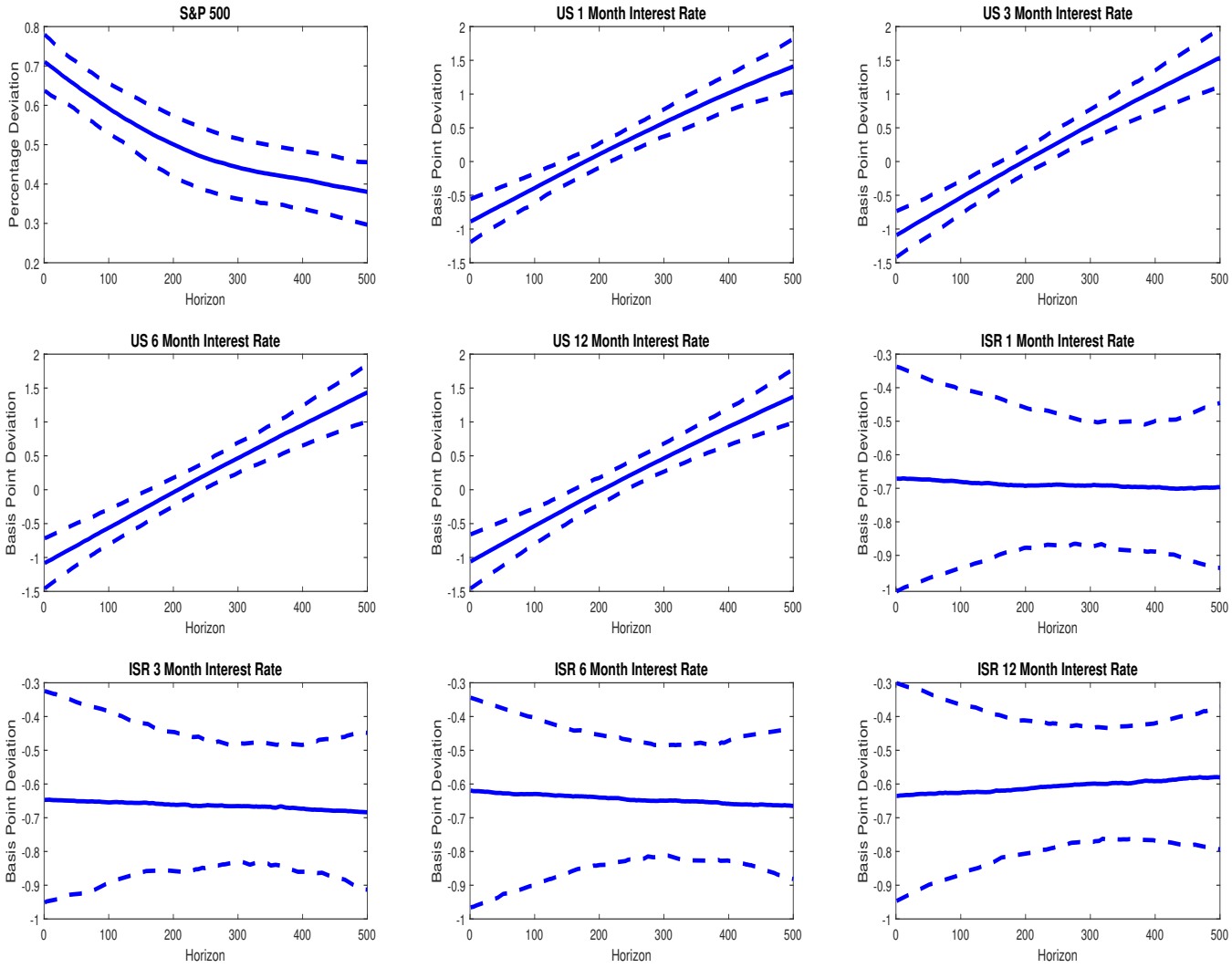

Notes: This figure presents the impulse responses of the S&P 500 index and 1-, 3-, 6-, and 12-month U.S. (Libor) and Israeli (Telbor) interest rates to a one standard deviation S&P 500 index innovation from replacing MSCI return with S&P 500 return in the model described by Equations (1) and (2) from the text. Responses are in terms of deviations from pre-shock values (percentage deviation for stock prices and basis point deviation for interest rates). Horizon (on x-axis) is in days.

Figure D.7: **FX Market Prices and Quantities: Replacing MSCI Return with S&P 500 Return: (a) Impulse Responses; (b) FEVs**.

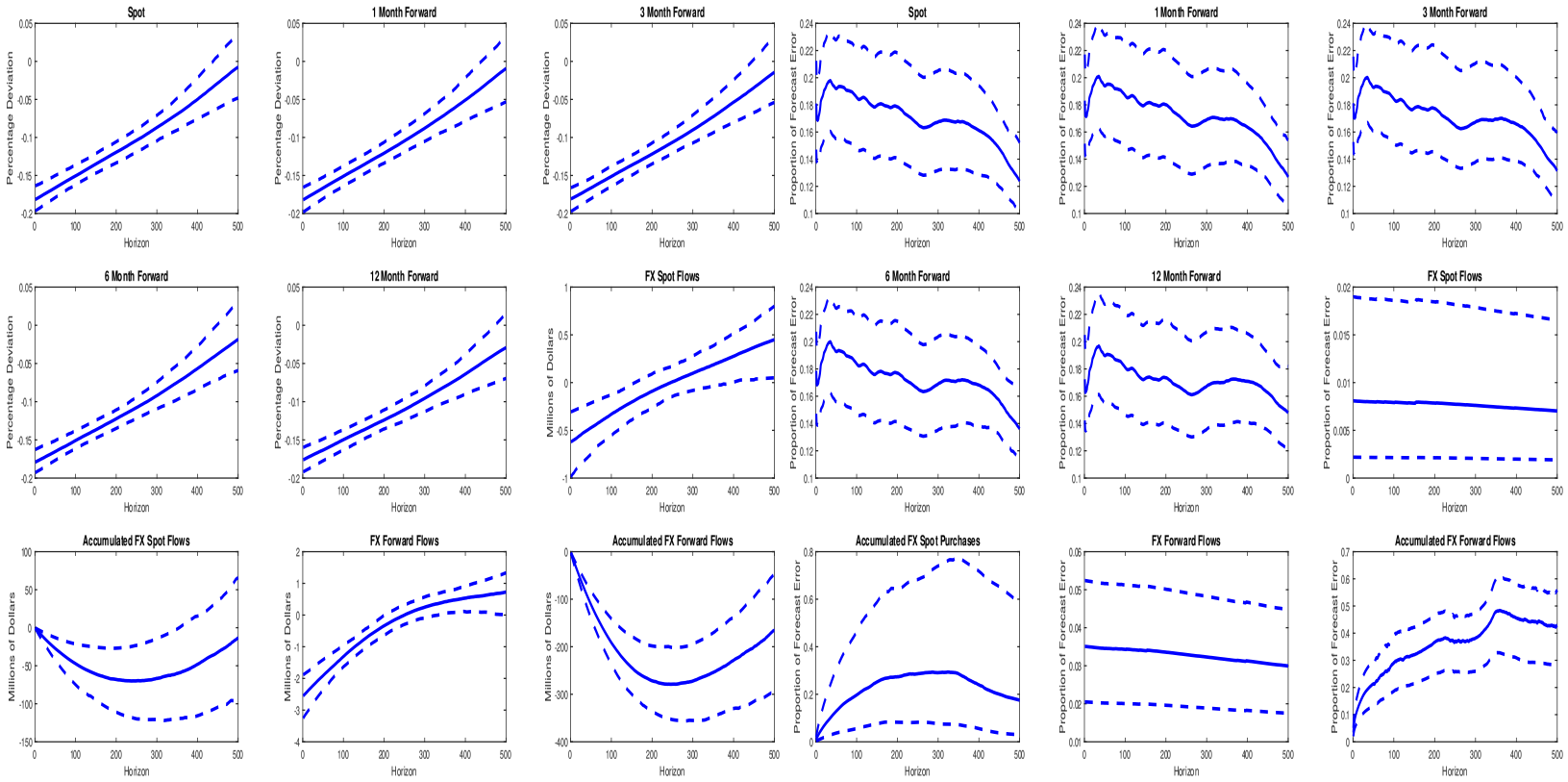

(a) Impulse Responses of FX Market Prices and Quantities to a One Standard Deviation MSCI Index Innovation.

(b) FEV of FX Market Prices and Quantities Attributable to MSCI Index Innovation.

Notes: Panel (a): This figure presents the impulse responses of the spot and forward rates and quantities to a one standard deviation S&p 500 index innovation from replacing MSCI return with S&P 500 return in the model described by Equations (1) and (2) from the text. Responses are in terms of deviations from pre-shock values (percentage deviation for spot and forward rates and Millions of dollars for spot and forward flows' raw and accumulated responses). Horizon (on x-axis) is in days. Panel (b): This figure presents the FEV share of the spot and forward rates and quantities that is attributable to the S&P 500 index innovation. Horizon is in days.

Figure D.8: **Impulse Responses to a One Standard Deviation S&P 500 Index Innovation: Non-II Sectors' Spot and Forward Flows**.

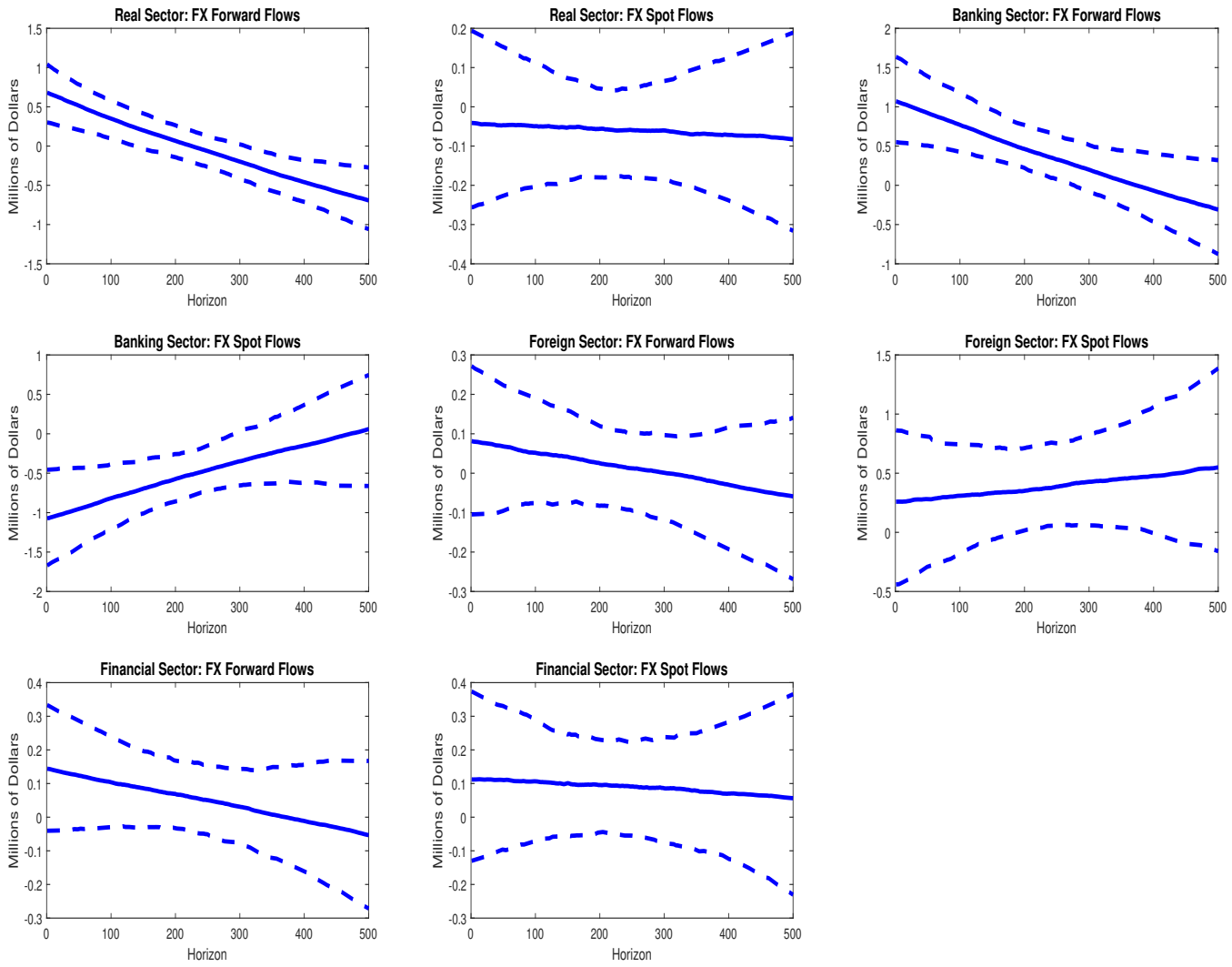

Notes: This figure presents the impulse responses of spot and forward flows of the real, banking, foreign, and financial sectors to a one standard deviation S&P 500 index innovation from replacing MSCI return with S&P 500 return in the model described by Equations (1) and (2) from the text. Responses are in terms of deviations from pre-shock values (in million of dollar terms). Horizon (on x-axis) is in days.

Figure D.9: **Impulse Responses to a One Standard Deviation S&P 500 Index Innovation: Banking and Real Sectors' Forward Flows Versus IIs' Forward Flows**.

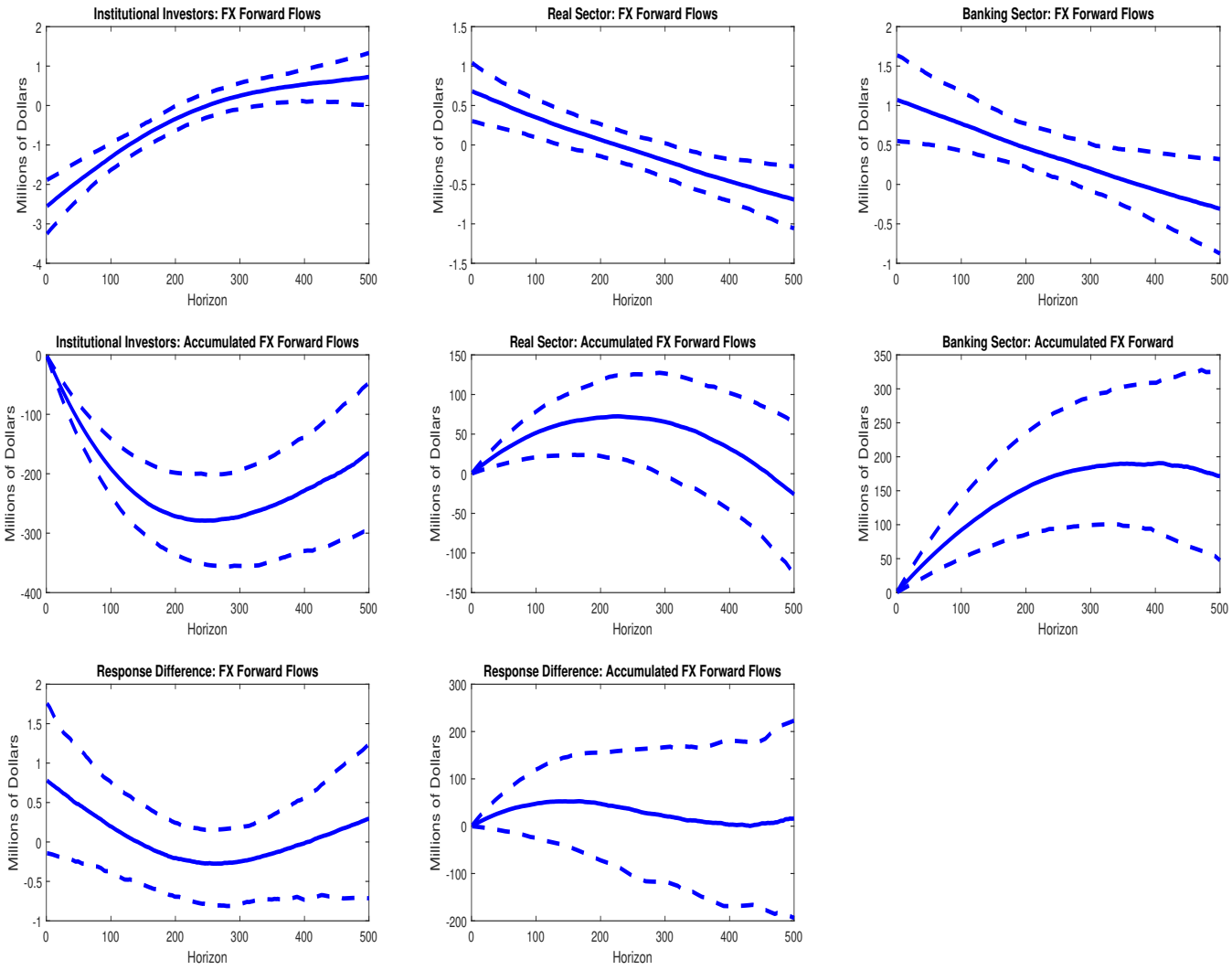

Notes: This figure presents the difference between raw and accumulated (in absolute terms) response of IIs' forward flows and the summed responses of the banking and real sectors' raw and accumulated forward flows, respectively, to a one standard deviation S&P 500 index innovation from replacing MSCI return with S&P 500 return in the model described by Equations (1) and (2) from the text. (For completeness, responses themselves (both raw and accumulated) for all three sectors are also shown in the figure.) Responses are in terms of deviations from pre-shock values (in million of dollar terms). Horizon (on x-axis) is in days.

Figure D.10: **Impulse Responses to a One Standard Deviation S&P 500 Index Innovation: Interest Rate Spreads and Cross-Currency Basis**.

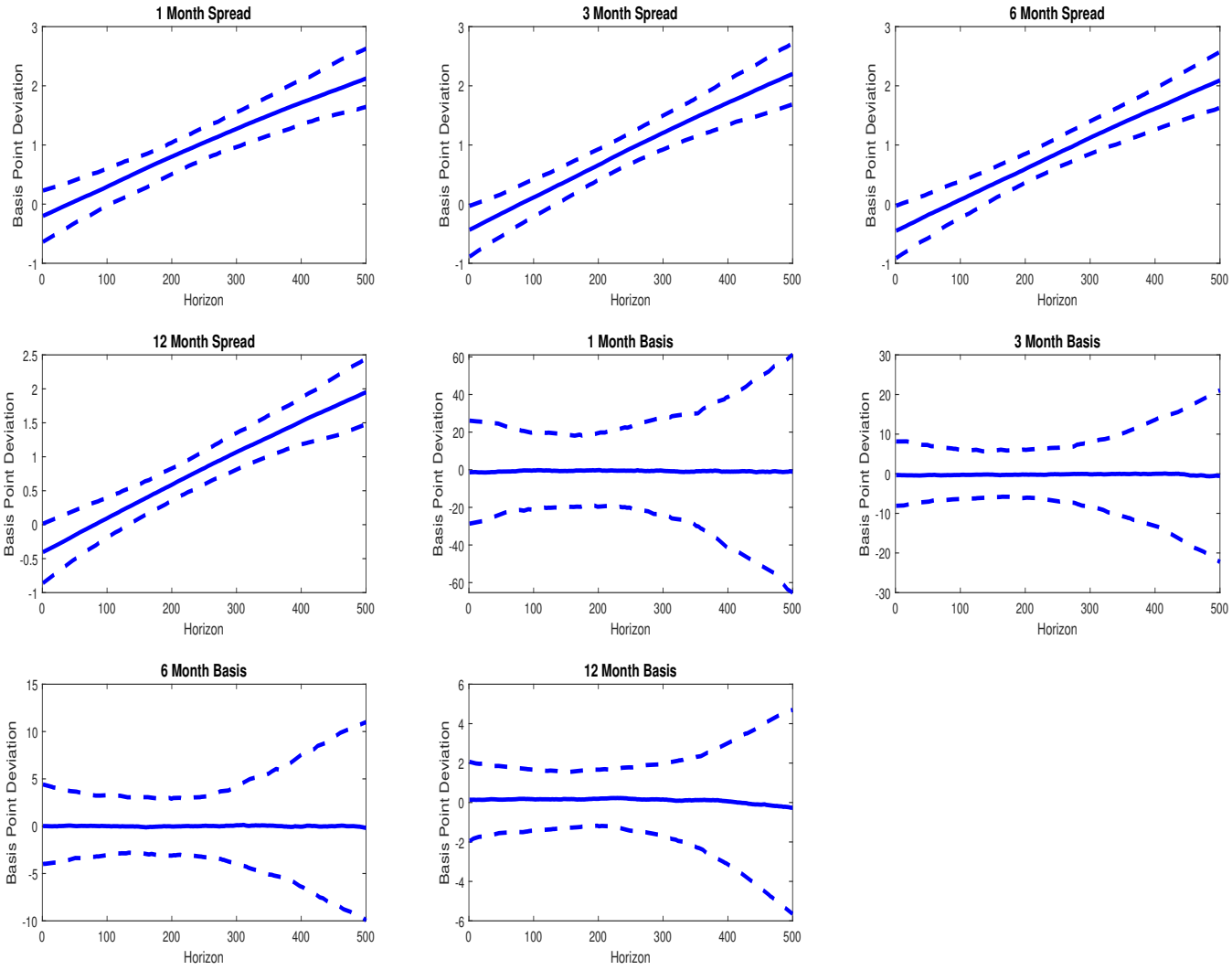

Notes: This figure presents the impulse response differences across U.S. (Libor) and Israeli (Telbor) interest rate responses and the associated USD/ILS cross-currency basis responses to a one standard deviation S&P 500 index innovation from replacing MSCI return with S&P 500 return in the model described by Equations (1) and (2) from the text. Responses are in terms of basis point deviation from pre-shock values. Horizon is in days.

Figure D.11: **Impulse Responses to a One Standard Deviation MSCI Index Innovation: MSCI and Interest Rates: Excluding the COVID-19-Related Period**.

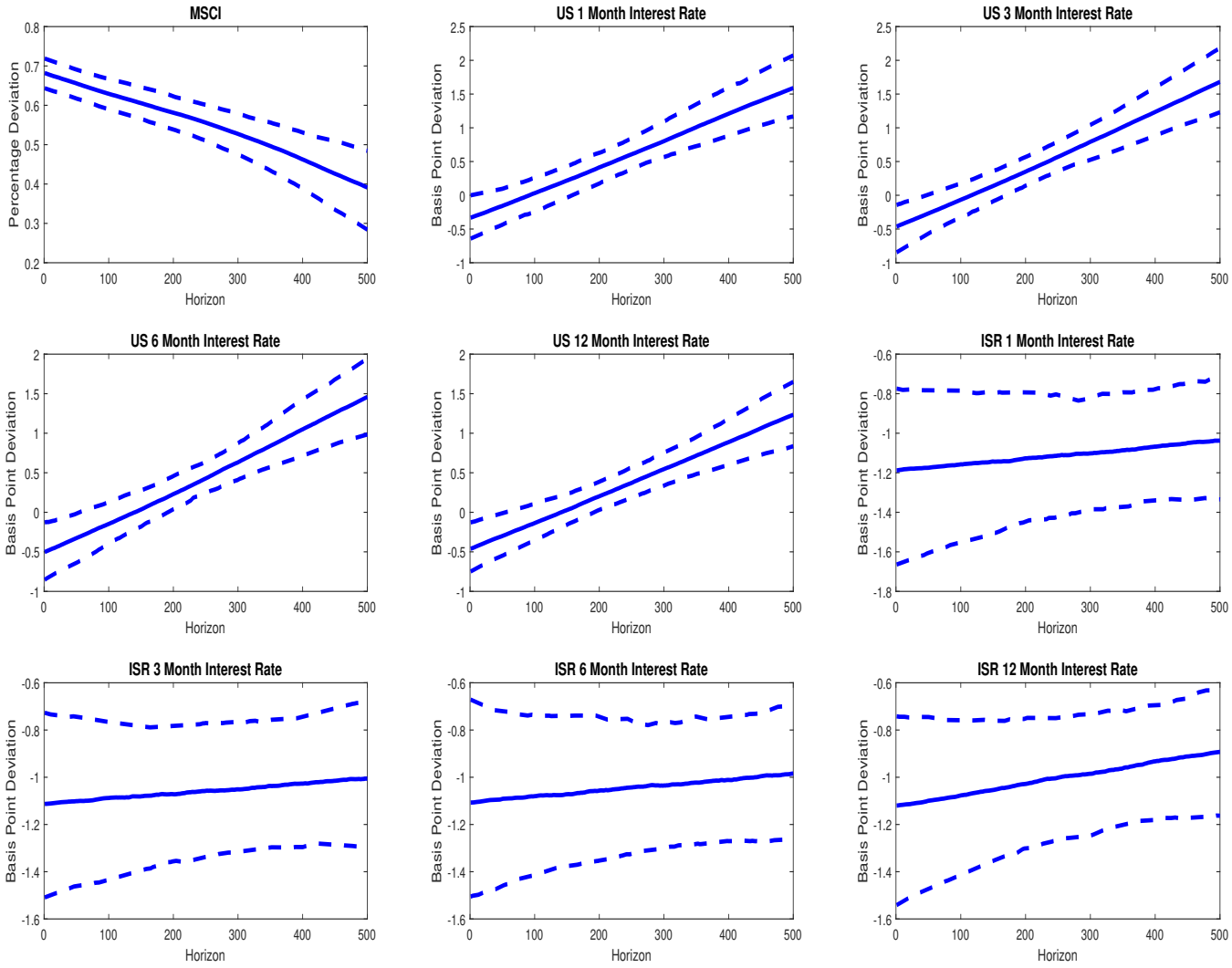

Notes: This figure presents the impulse responses of MSCI and 1-, 3-, 6-, and 12-month U.S. (Libor) and Israeli (Telbor) interest rates to a one standard deviation MSCI index innovation from the model described by Equations (1) and (2) from the text, where the baseline sample is truncated at February 19, 2020. Responses are in terms of deviations from pre-shock values (percentage deviation for stock prices and basis point deviation for interest rates). Horizon (on x-axis) is in days.

Figure D.12: **FX Market Prices and Quantities: Excluding the COVID-19-Related Period: (a) Impulse Responses; (b) FEVs**.

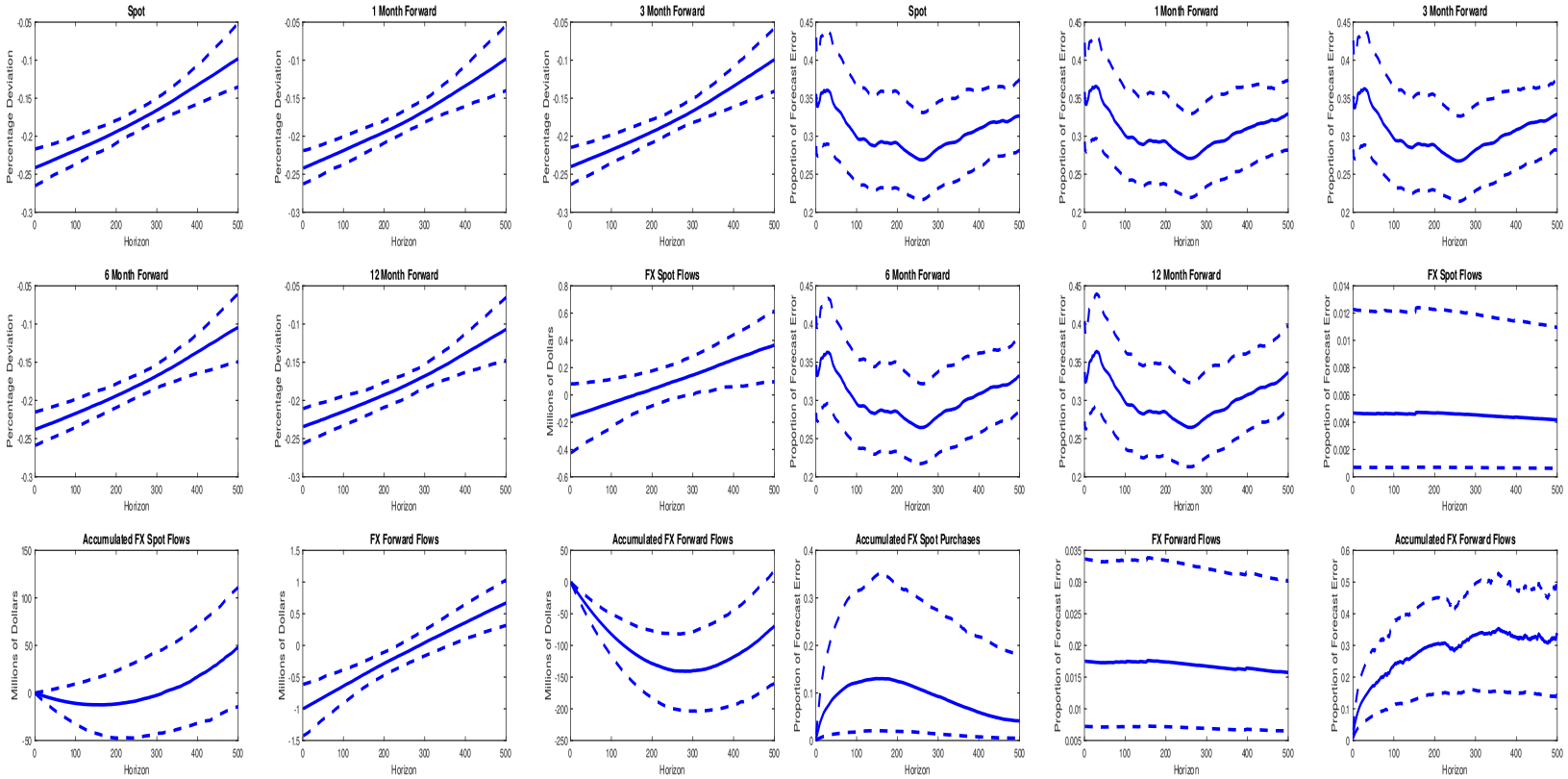

(a) Impulse Responses of FX Market Prices and Quantities to a One Standard Deviation MSCI Index Innovation.

(b) FEV of FX Market Prices and Quantities Attributable to MSCI Index Innovation.

Notes: Panel (a): This figure presents the impulse responses of the spot and forward rates and quantities to a one standard deviation MSCI index innovation from the model described by Equations (1) and (2) from the text, where the baseline sample is truncated at February 19, 2020. Responses are in terms of deviations from pre-shock values (percentage deviation for spot and forward rates and Millions of dollars for spot and forward flows' raw and accumulated responses). Horizon (on x-axis) is in days. Panel (b): This figure presents the FEV share of the spot and forward rates and quantities that is attributable to the MSCI index innovation from the model described by Equations (1) and (2) from the text, where the baseline sample is truncated at February 19, 2020. Horizon is in days.

Figure D.13: **Impulse Responses to a One Standard Deviation MSCI Index Innovation: Non-II Sectors' Spot and Forward Flows: Excluding the COVID-19-Related Period**.

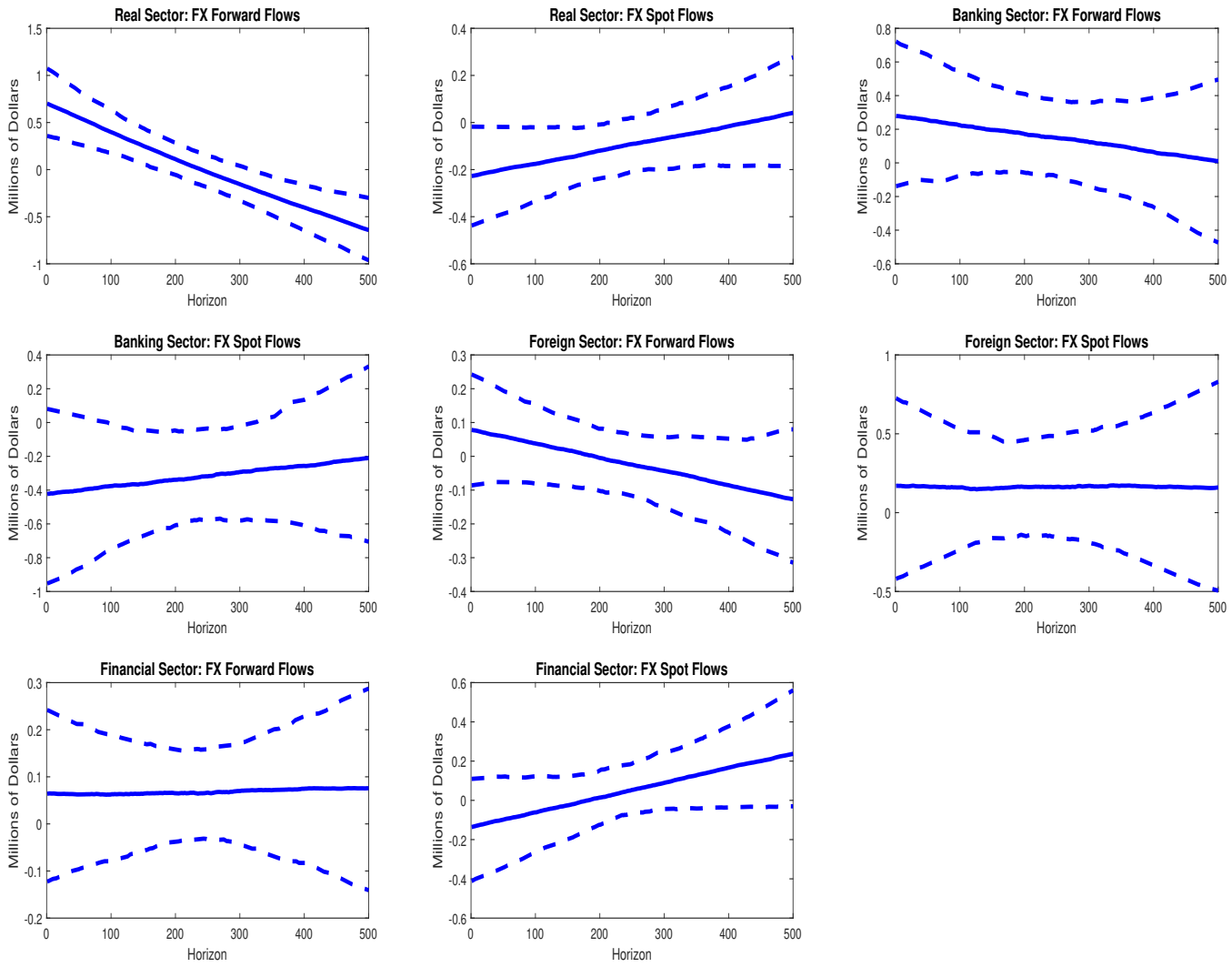

Notes: This figure presents the impulse responses of spot and forward flows of the real, banking, foreign, and financial sectors to a one standard deviation MSCI index innovation from the model described by Equations (1) and (2) from the text, where the baseline sample is truncated at February 19, 2020. Responses are in terms of deviations from pre-shock values (in million of dollar terms). Horizon (on x-axis) is in days.

Figure D.14: **Impulse Responses to a One Standard Deviation MSCI Index Innovation: Banking and Real Sectors' Forward Flows Versus IIs' Forward Flows: Excluding the COVID-19-Related Period**.

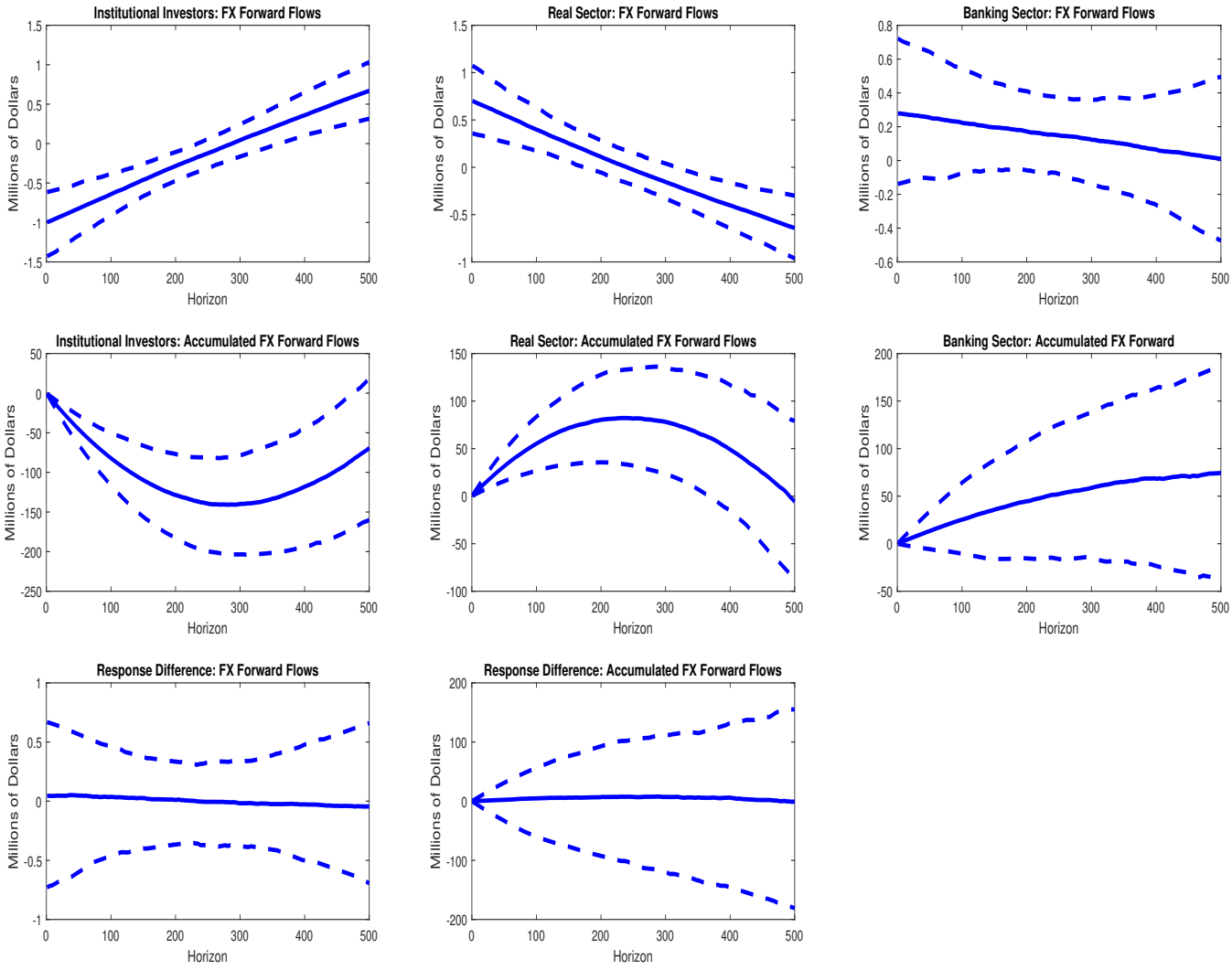

Notes: This figure presents the difference between raw and accumulated (in absolute terms) response of IIs' forward flows and the summed responses of the banking and real sectors' raw and accumulated forward flows, respectively, to a one standard deviation MSCI index innovation from the model described by Equations (1) and (2) from the text, where the baseline sample is truncated at February 19, 2020. (For completeness, responses themselves (both raw and accumulated) for all three sectors are also shown in the figure.) Responses are in terms of deviations from pre-shock values (in million of dollar terms). Horizon (on x-axis) is in days.

Figure D.15: **Impulse Responses to a One Standard Deviation MSCI Index Innovation: Interest Rate Spreads and Cross-Currency Basis: Excluding the COVID-19-Related Period**.

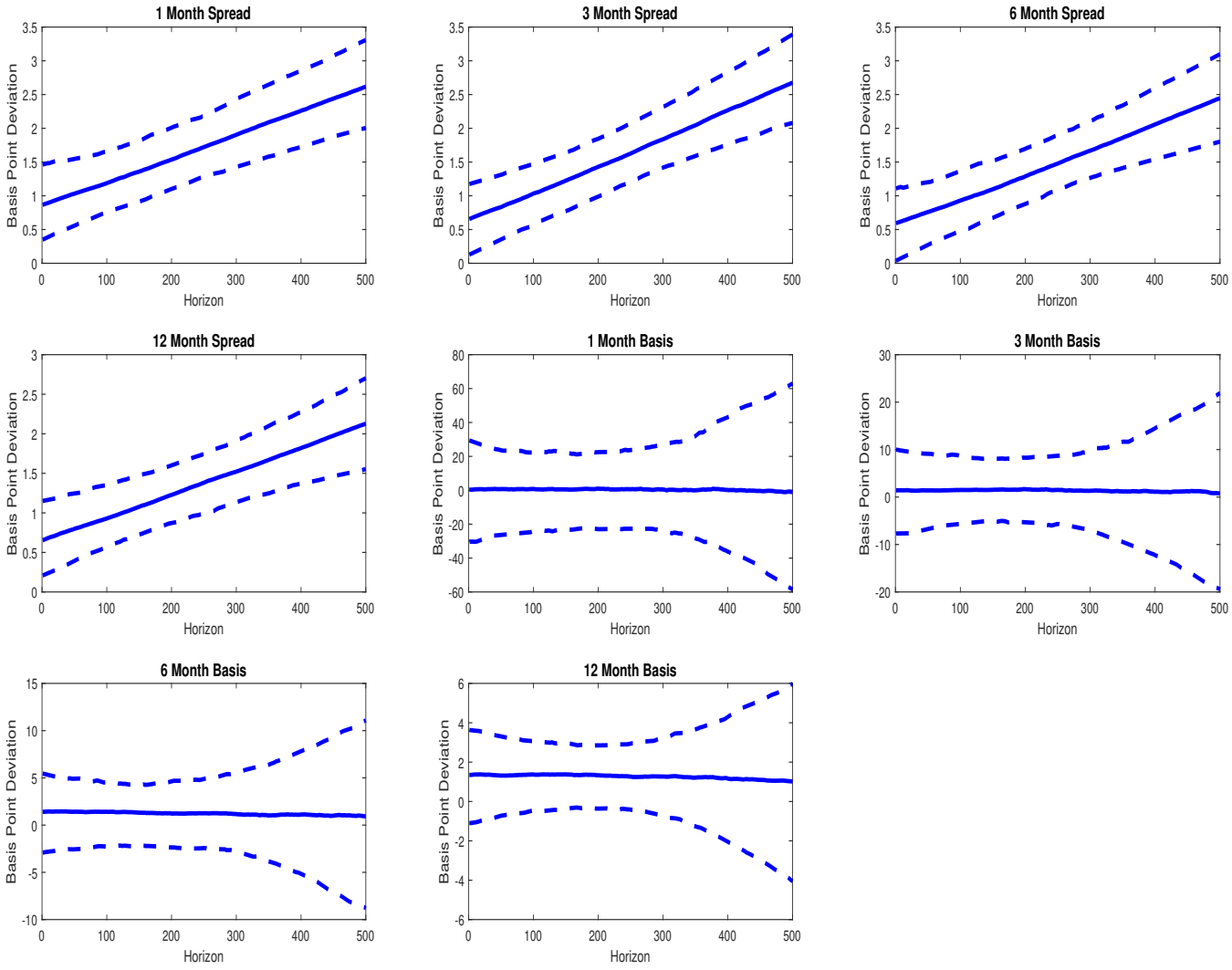

Notes: This figure presents the impulse response differences across U.S. (Libor) and Israeli (Telbor) interest rate responses and the associated USD/ILS cross-currency basis responses to a one standard deviation MSCI index innovation from the model described by Equations (1) and (2) from the text, where the baseline sample is truncated at February 19, 2020. Responses are in terms of basis point deviation from pre-shock values. Horizon is in days.

Figure D.16: **Impulse Responses to a One Standard Deviation MSCI Index Innovation: MSCI and Interest Rates: 10 Lags**.

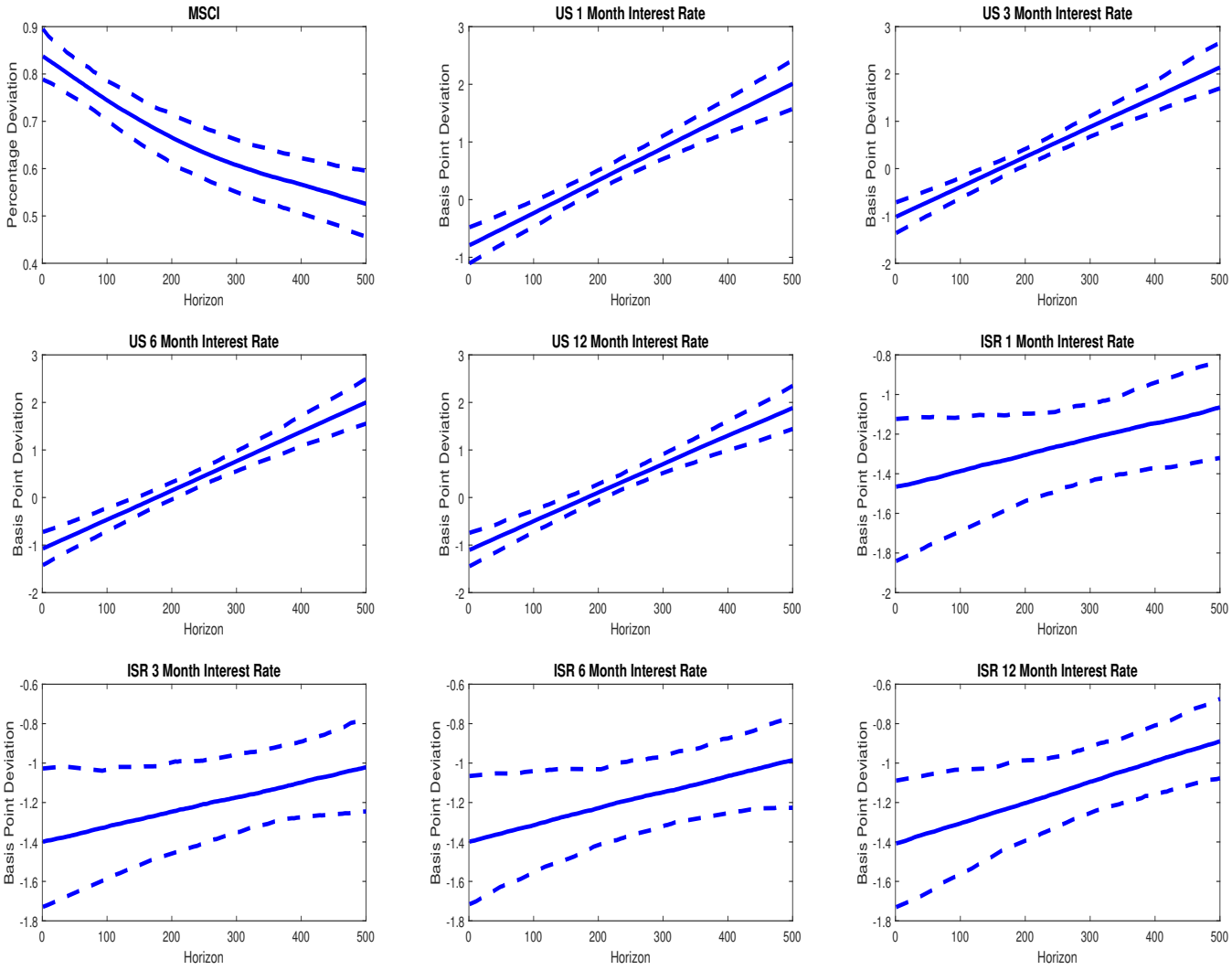

Notes: This figure presents the impulse responses of MSCI and 1-, 3-, 6-, and 12-month U.S. (Libor) and Israeli (Telbor) interest rates to a one standard deviation MSCI index innovation from the model described by Equations (1) and (2) from the text, where a 30-lag specification is assumed in Equation (1) instead of the baseline 20-lag specification. Responses are in terms of deviations from pre-shock values (percentage deviation for stock prices and basis point deviation for interest rates). Horizon (on x-axis) is in days.

Figure D.17: **FX Market Prices and Quantities: 10 Lags: (a) Impulse Responses; (b) FEVs.**

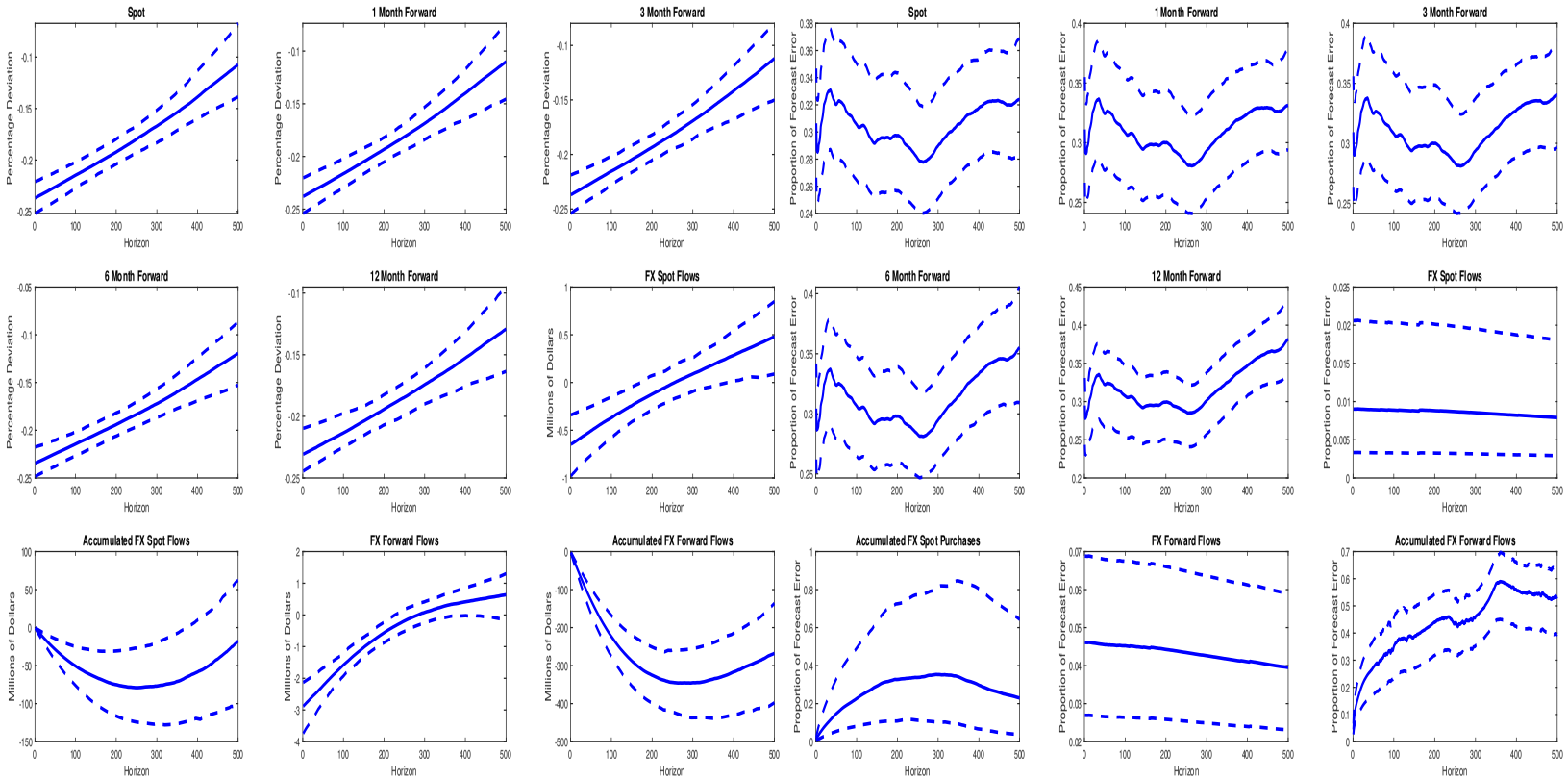

(a) Impulse Responses of FX Market Prices and Quantities to a One Standard Deviation MSCI Index Innovation.

(b) FEV of FX Market Prices and Quantities Attributable to MSCI Index Innovation.

Notes: Panel (a): This figure presents the impulse responses of the spot and forward rates and quantities to a one standard deviation MSCI index innovation from the model described by Equations (1) and (2) from the text, where a 30-lag specification is assumed in Equation (1) instead of the baseline 20-lag specification. Responses are in terms of deviations from pre-shock values (percentage deviation for spot and forward rates and Millions of dollars for spot and forward flows, spot-flows-induced accumulated spot FX purchases, and forward-flows-induced accumulated short position). Horizon (on x-axis) is in days. Panel (b): This figure presents the FEV share of the spot and forward rates and quantities that is attributable to the MSCI index innovation from the model described by Equations (1) and (2) from the text, where a 30-lag specification is assumed in Equation (1) instead of the baseline 20-lag specification. Horizon is in days.

Figure D.18: **Impulse Responses to a One Standard Deviation MSCI Index Innovation: Non-II Sectors' Spot and Forward Flows: 10 Lags**.

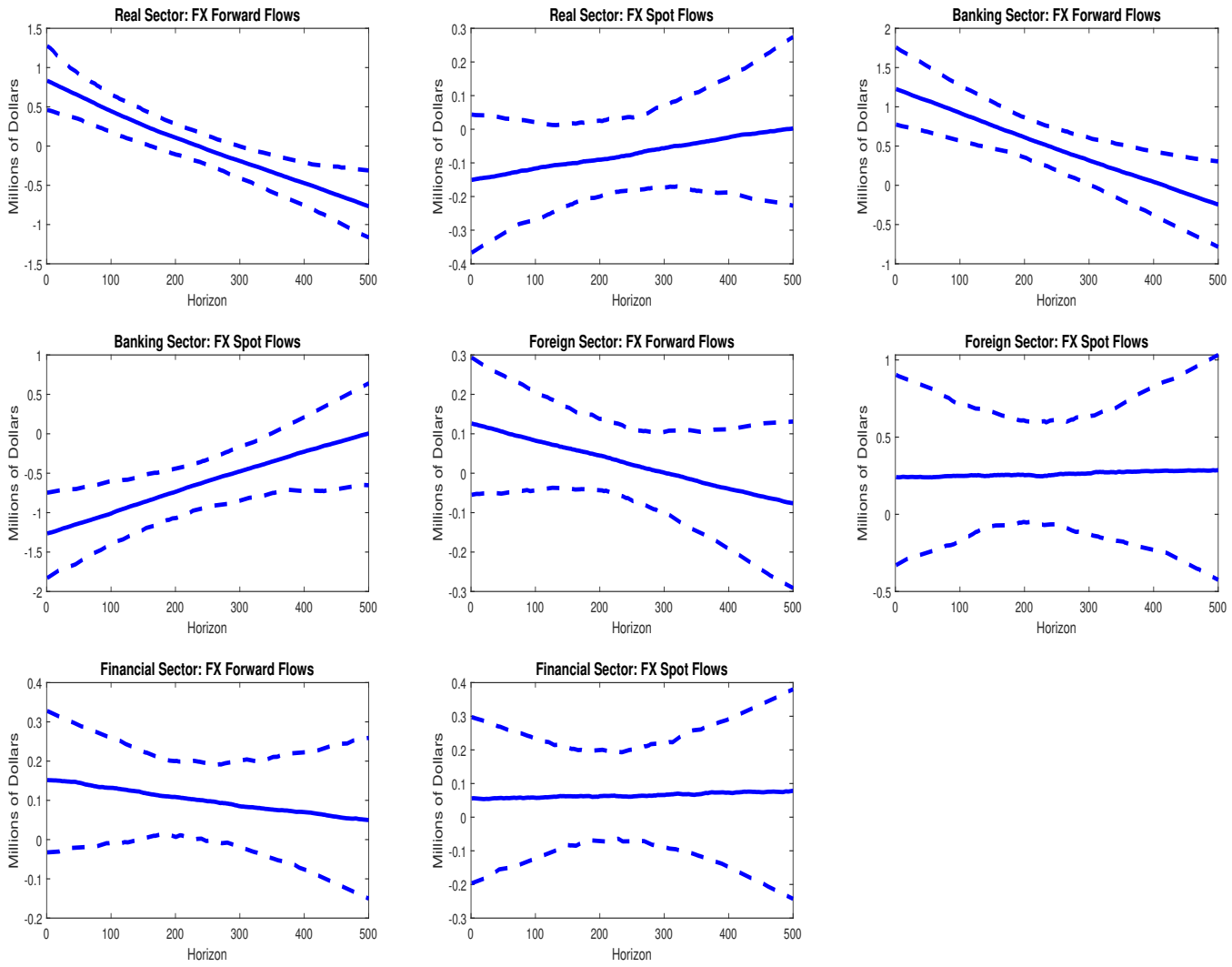

Notes: This figure presents the impulse responses of spot and forward flows of the real, banking, foreign, and financial sectors to a one standard deviation MSCI index innovation from the model described by Equations (1) and (2) from the text, where a 30-lag specification is assumed in Equation (1) instead of the baseline 20-lag specification. Responses are in terms of deviations from pre-shock values (in million of dollar terms). Horizon (on x-axis) is in days.

Figure D.19: **Impulse Responses to a One Standard Deviation MSCI Index Innovation: Banking and Real Sectors' Forward Flows Versus IIs' Forward Flows: 10 Lags**.

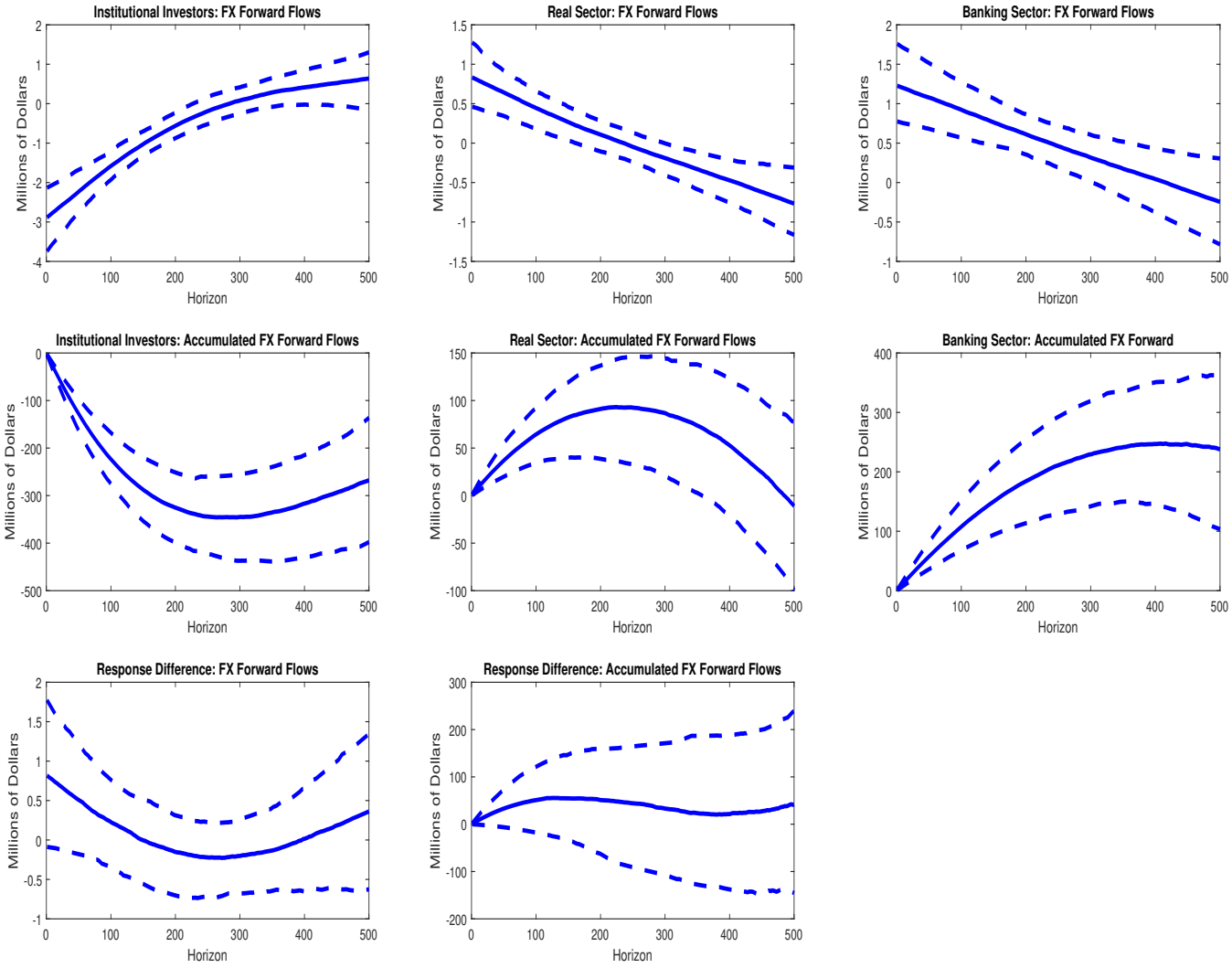

Notes: This figure presents the difference between raw and accumulated (in absolute terms) response of IIs' forward flows and the summed responses of the banking and real sectors' raw and accumulated forward flows, respectively, to a one standard deviation MSCI index innovation from the model described by Equations (1) and (2) from the text, where a 30-lag specification is assumed in Equation (1) instead of the baseline 20-lag specification. (For completeness, responses themselves (both raw and accumulated) for all three sectors are also shown in the figure.) Responses are in terms of deviations from pre-shock values (in million of dollar terms). Horizon (on x-axis) is in days.

Figure D.20: **Impulse Responses to a One Standard Deviation MSCI Index Innovation: Interest Rate Spreads and Cross-Currency Basis: 10 Lags**.

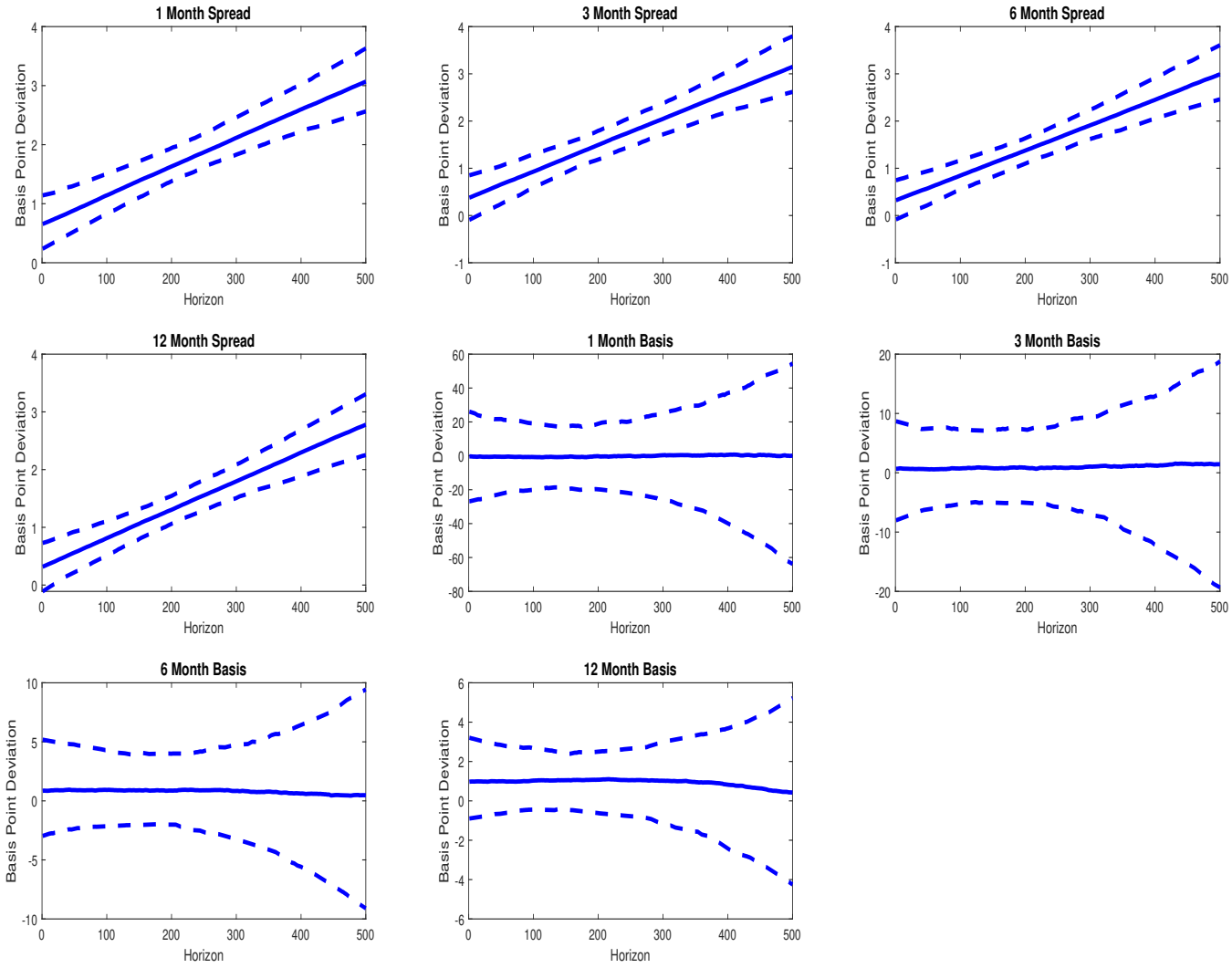

Notes: This figure presents the impulse response differences across U.S. (Libor) and Israeli (Telbor) interest rate responses and the associated USD/ILS cross-currency basis responses to a one standard deviation MSCI index innovation from the model described by Equations (1) and (2) from the text, where a 30-lag specification is assumed in Equation (1) instead of the baseline 20-lag specification. Responses are in terms of basis point deviation from pre-shock values. Horizon is in days.

Figure D.21: **Impulse Responses to a One Standard Deviation MSCI Index Innovation: MSCI and Interest Rates: 30 Lags**.

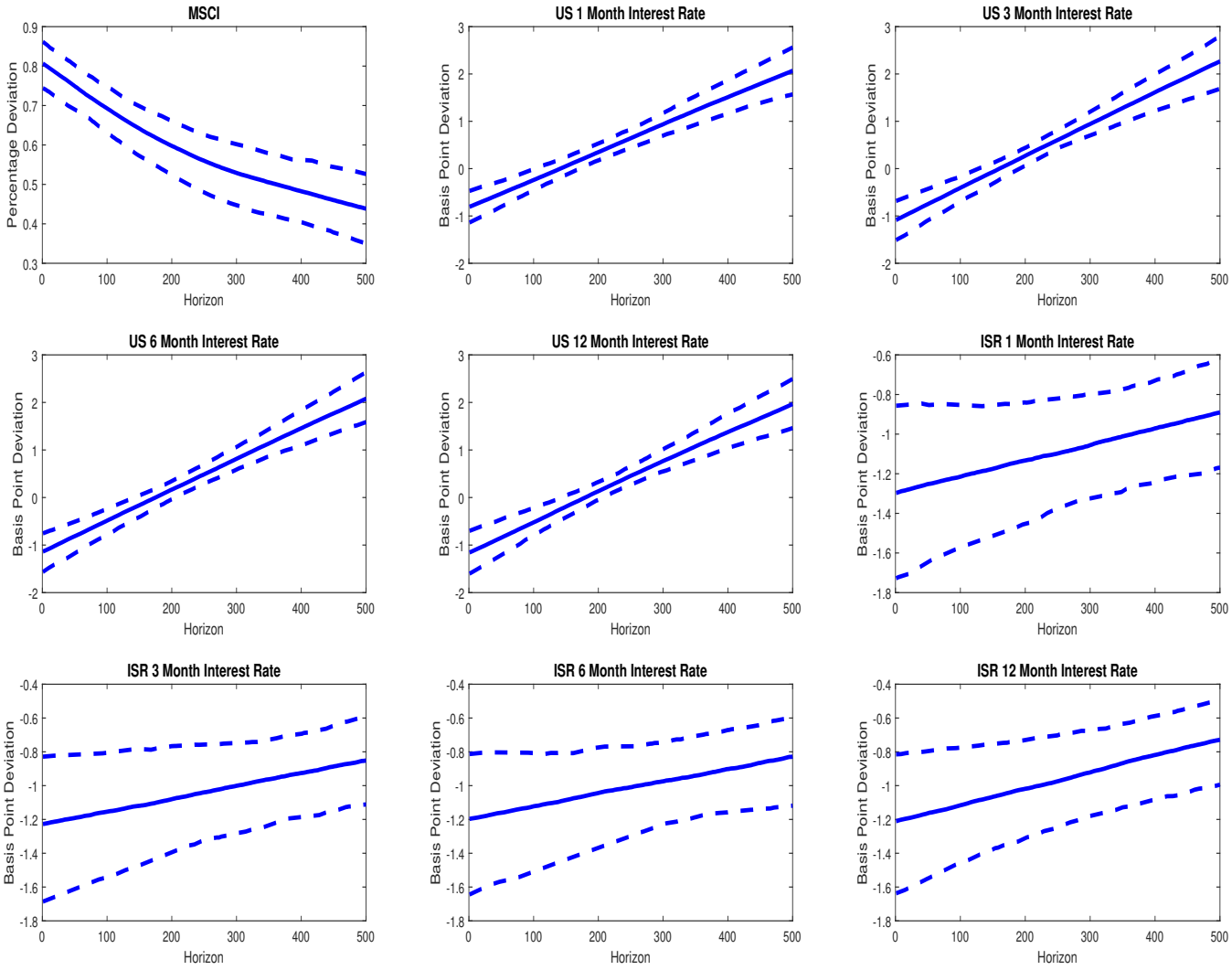

Notes: This figure presents the impulse responses of MSCI and 1-, 3-, 6-, and 12-month U.S. (Libor) and Israeli (Telbor) interest rates to a one standard deviation MSCI index innovation from the model described by Equations (1) and (2) from the text, where a 30-lag specification is assumed in Equation (1) instead of the baseline 20-lag specification. Responses are in terms of deviations from pre-shock values (percentage deviation for stock prices and basis point deviation for interest rates). Horizon (on x-axis) is in days.

Figure D.22: **FX Market Prices and Quantities: 30 Lags: (a) Impulse Responses; (b) FEVs.**

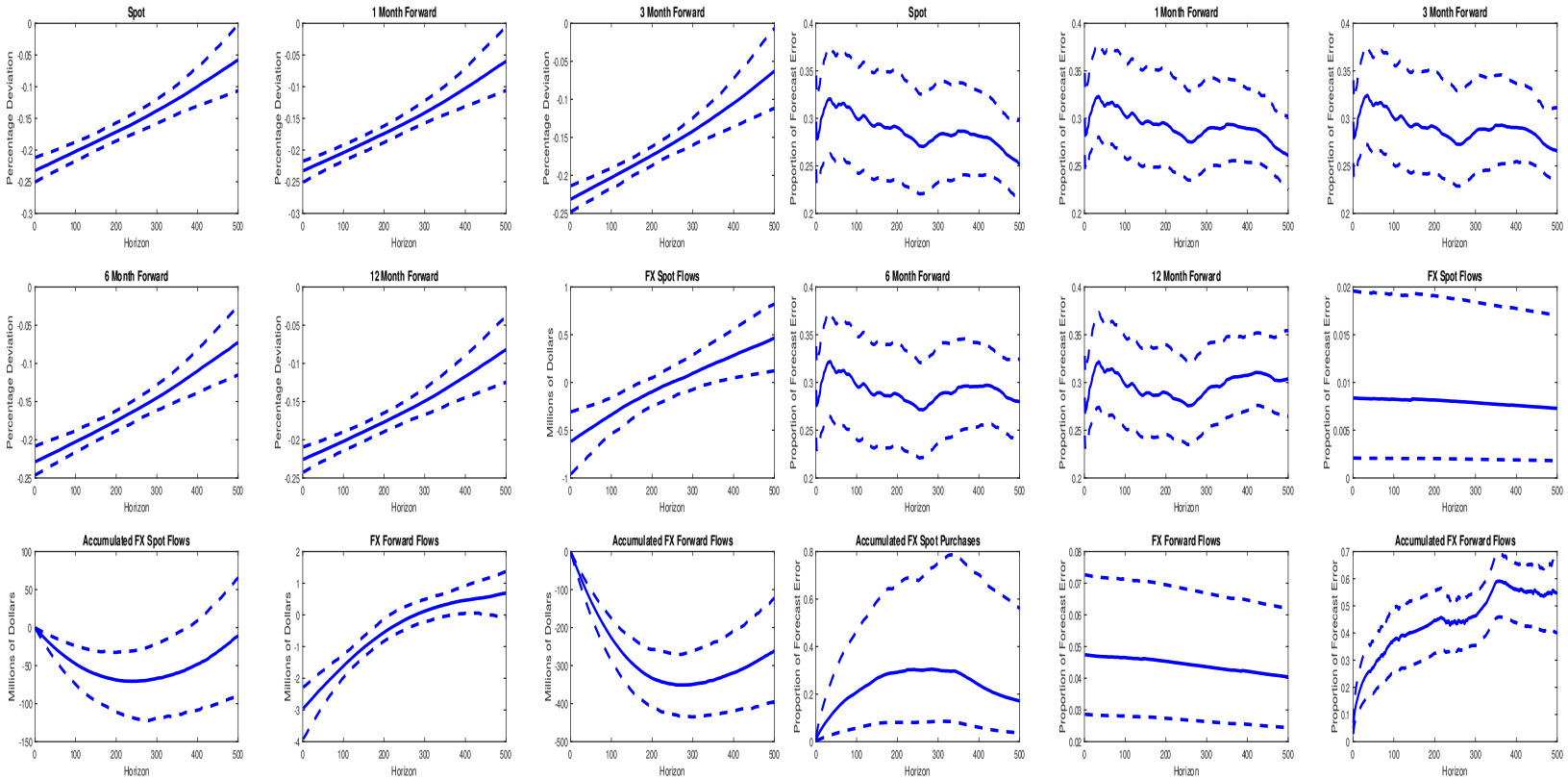

(a) Impulse Responses of FX Market Prices and Quantities to a One Standard Deviation MSCI Index Innovation.

(b) FEV of FX Market Prices and Quantities Attributable to MSCI Index Innovation.

Notes: Panel (a): This figure presents the impulse responses of the spot and forward rates and quantities to a one standard deviation MSCI index innovation from the model described by Equations (1) and (2) from the text, where a 30-lag specification is assumed in Equation (1) instead of the baseline 20-lag specification. Responses are in terms of deviations from pre-shock values (percentage deviation for spot and forward rates and Millions of dollars for spot and forward flows, spot-flows-induced accumulated spot FX purchases, and forward-flows-induced accumulated short position). Horizon (on x-axis) is in days. Panel (b): This figure presents the FEV share of the spot and forward rates and quantities that is attributable to the MSCI index innovation from the model described by Equations (1) and (2) from the text, where a 30-lag specification is assumed in Equation (1) instead of the baseline 20-lag specification. Horizon is in days.

Figure D.23: **Impulse Responses to a One Standard Deviation MSCI Index Innovation: Non-II Sectors' Spot and Forward Flows: 30 Lags**.

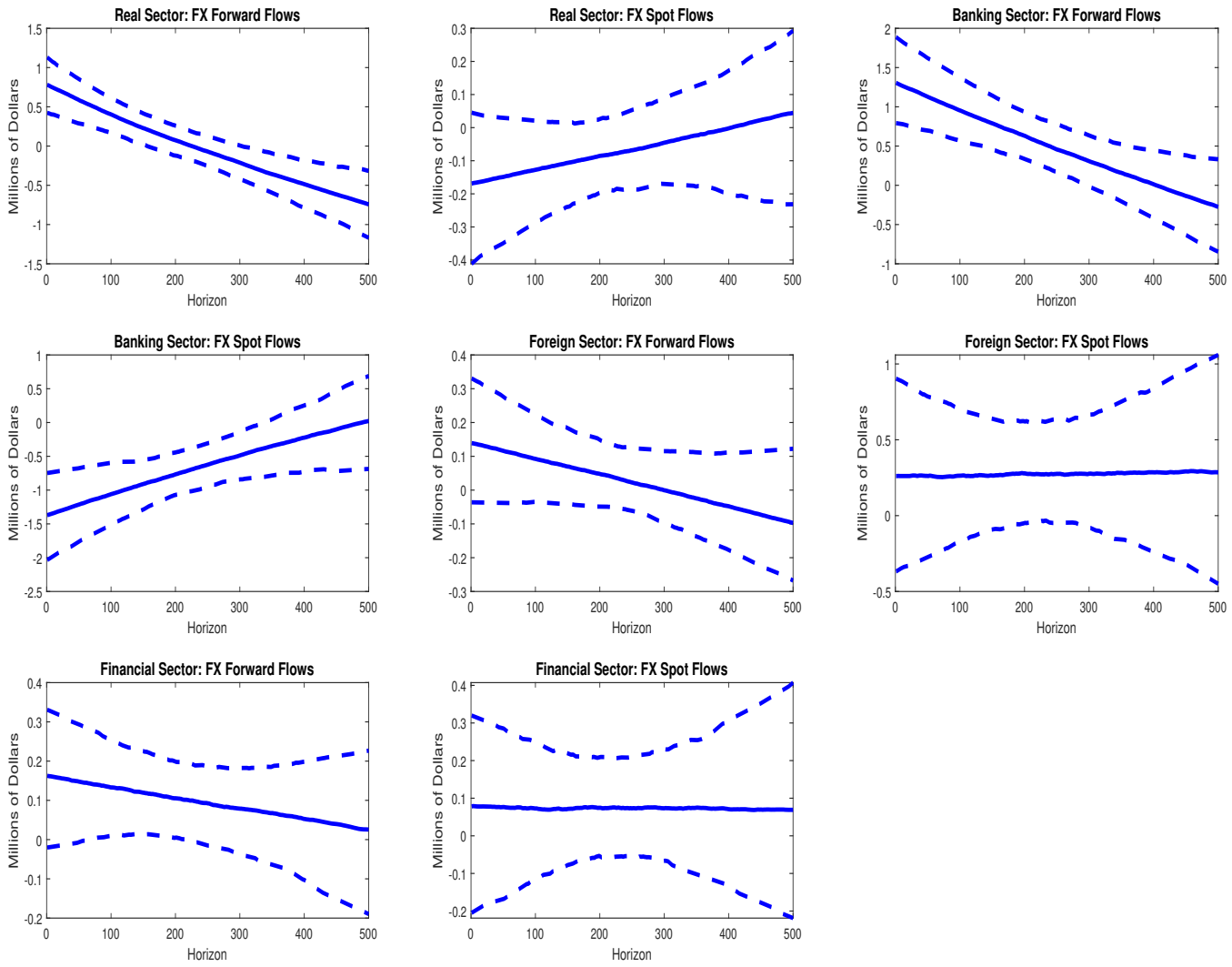

Notes: This figure presents the impulse responses of spot and forward flows of the real, banking, foreign, and financial sectors to a one standard deviation MSCI index innovation from the model described by Equations (1) and (2) from the text, where a 30-lag specification is assumed in Equation (1) instead of the baseline 20-lag specification. Responses are in terms of deviations from pre-shock values (in million of dollar terms). Horizon (on x-axis) is in days.

Figure D.24: **Impulse Responses to a One Standard Deviation MSCI Index Innovation: Banking and Real Sectors' Forward Flows Versus IIs' Forward Flows: 30 Lags**.

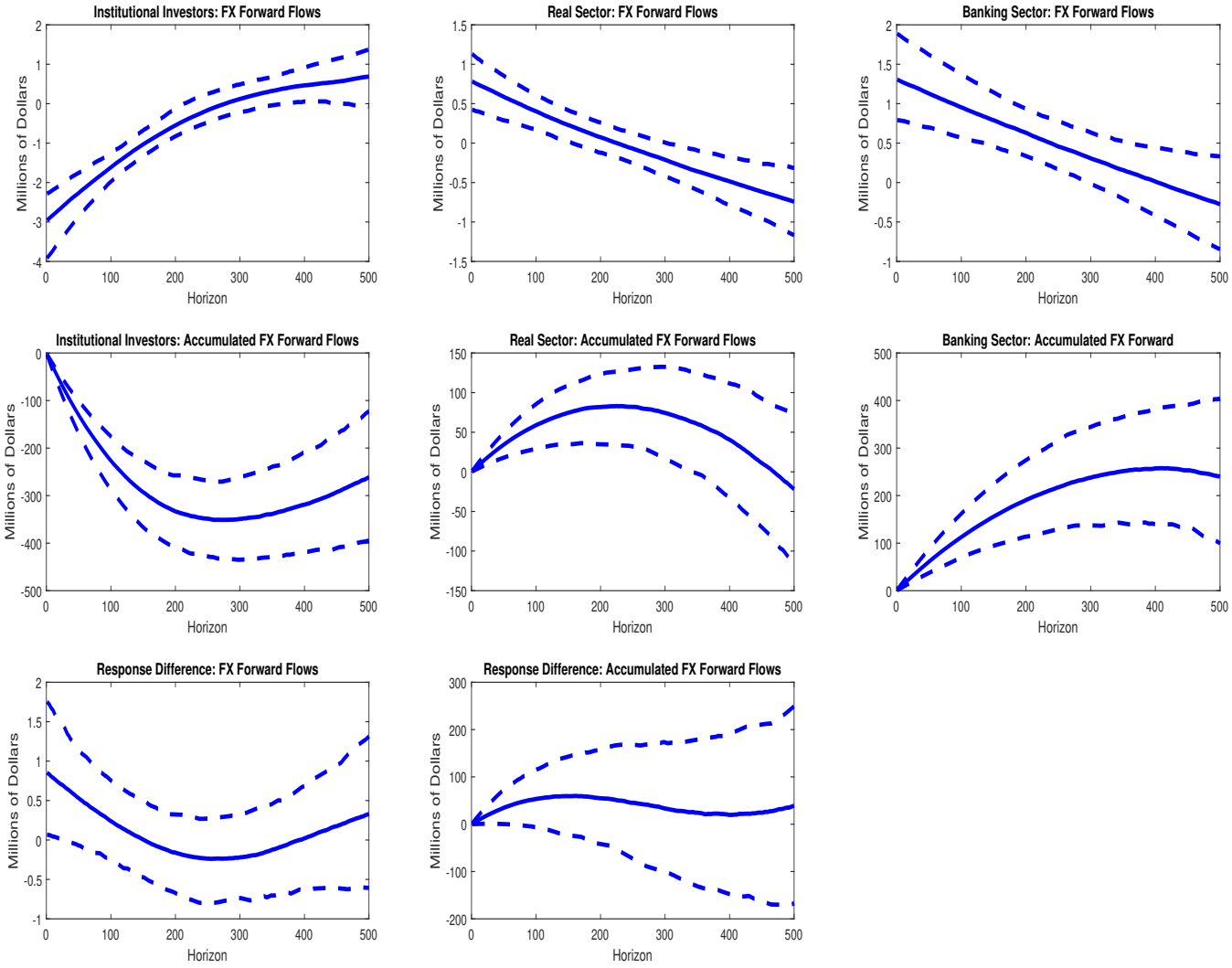

Notes: This figure presents the difference between raw and accumulated (in absolute terms) response of IIs' forward flows and the summed responses of the banking and real sectors' raw and accumulated forward flows, respectively, to a one standard deviation MSCI index innovation from the model described by Equations (1) and (2) from the text, where a 30-lag specification is assumed in Equation (1) instead of the baseline 20-lag specification. (For completeness, responses themselves (both raw and accumulated) for all three sectors are also shown in the figure.) Responses are in terms of deviations from pre-shock values (in million of dollar terms). Horizon (on x-axis) is in days.

Figure D.25: **Impulse Responses to a One Standard Deviation MSCI Index Innovation: Interest Rate Spreads and Cross-Currency Basis: 30 Lags**.

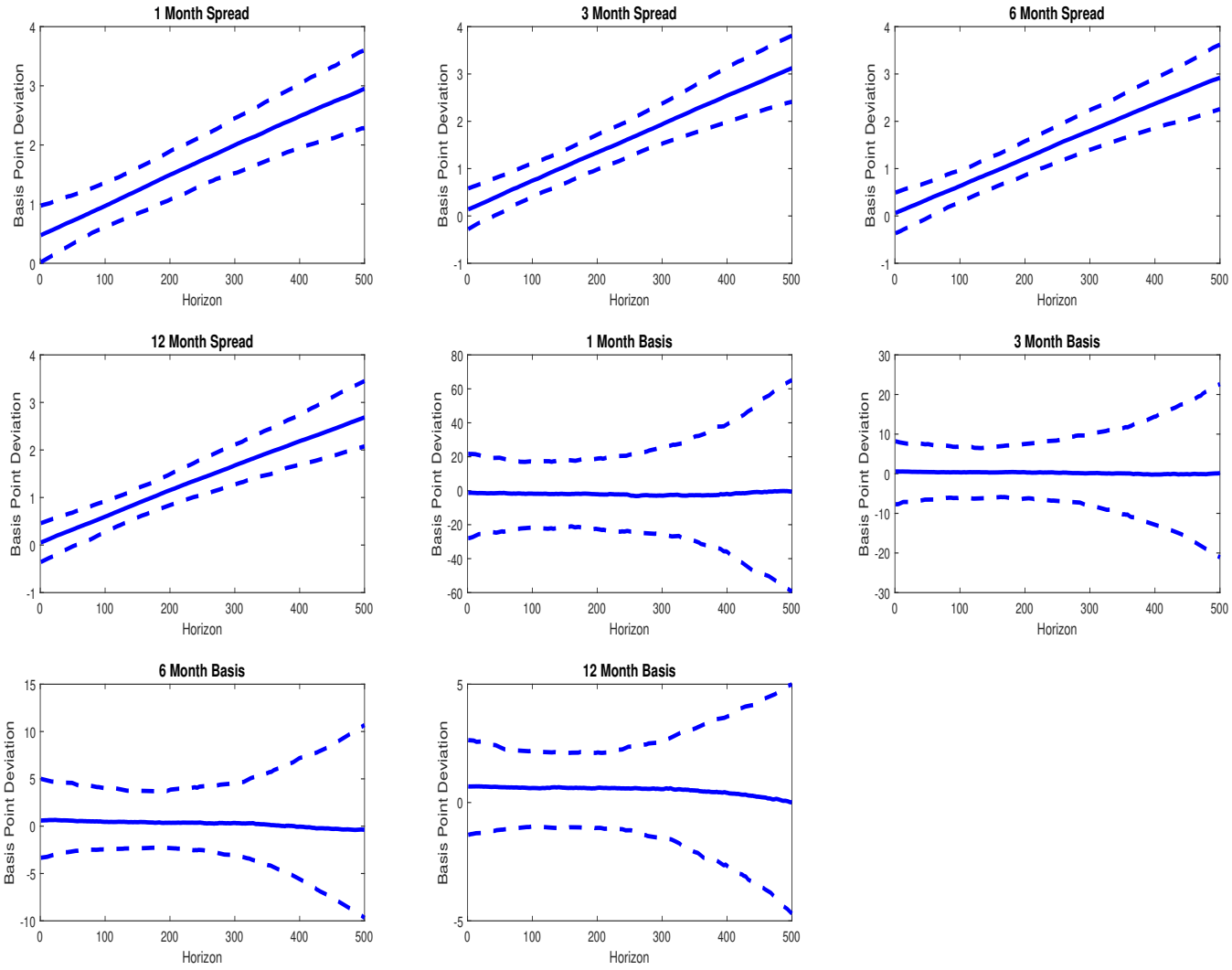

Notes: This figure presents the impulse response differences across U.S. (Libor) and Israeli (Telbor) interest rate responses and the associated USD/ILS cross-currency basis responses to a one standard deviation MSCI index innovation from the model described by Equations (1) and (2) from the text, where a 30-lag specification is assumed in Equation (1) instead of the baseline 20-lag specification. Responses are in terms of basis point deviation from pre-shock values. Horizon is in days.

References

Alvarez, F. and Lippi, F.: 2022, The analytic theory of a monetary shock, *Econometrica* **90**(4), 1655–1680.

Barnichon, R. and Brownlees, C.: 2019, Impulse Response Estimation by Smooth Local Projections, *The Review of Economics and Statistics* **101**(3), 522–530.

Cornea-Madeira, A.: 2017, The Explicit Formula for the Hodrick-Prescott Filter in a Finite Sample, *The Review of Economics and Statistics* **99**(2), 314–318.

Du, W., Tepper, A. and Verdelhan, A.: 2018, Deviations from covered interest rate parity, *The Journal of Finance* **73**(3), 915–957.

Giannone, D., Lenza, M. and Primiceri, G. E.: 2015, Prior Selection for Vector Autoregressions, *The Review of Economics and Statistics* **97**(2), 436–451.

Gómez, V.: 1999, Three equivalent methods for filtering finite nonstationary time series, *Journal of Business & Economic Statistics* **17**(1), 109–116.

Hamilton, J. D.: 2018, Why You Should Never Use the Hodrick-Prescott Filter, *The Review of Economics and Statistics* **100**(5), 831–843.

Harvey, A. C.: 1990, *Forecasting, Structural Time Series Models and the Kalman Filter*, Cambridge University Press.

Hodrick, R. and Prescott, E.: 1997, Postwar u.s. business cycles: An empirical investigation, *Journal of Money, Credit and Banking* **29**(1), 1–16.

Ivashina, V., Scharfstein, D. S. and Stein, J. C.: 2015, Dollar Funding and the Lending Behavior of Global Banks, *The Quarterly Journal of Economics* **130**(3), 1241–1281.

Liao, G. Y. and Zhang, T.: 2020, The Hedging Channel of Exchange Rate Determination, *International Finance Discussion Papers 1283*, Board of Governors of the Federal Reserve System (U.S.).

Miranda-Agrippino, S. and Ricco, G.: 2021, The transmission of monetary policy shocks, *American Economic Journal: Macroeconomics* **13**(3), 74–107.

Müller, U. K.: 2013, Risk of bayesian inference in misspecified models, and the sandwich covariance matrix, *Econometrica* **81**(5), 1805–1849.

Plagborg-Møller, M.: 2019, Bayesian inference on structural impulse response functions, *Quantitative Economics* **10**(1), 145–184.

Plagborg-Møller, M.: 2016, *Essays in macroeconometrics*, Phd thesis, department of economics, harvard university.

Tanaka, M.: 2019, Bayesian inference of local projections with roughness penalty priors, *Computational Economics* **55**(2), 629–651.

Uhlig, H.: 1994, What macroeconomists should know about unit roots: A bayesian perspective, *Econometric Theory* **10**(3/4), 645–671.